The Geological Society of America | American Geophysical Union
Special Paper 514 | Special Publication 71
2015

The mantle isotopic printer: Basic mantle plume geochemistry for seismologists and geodynamicists

Michele Lustrino*
Dipartimento di Scienze della Terra, Università degli Studi di Roma La Sapienza, P.le A. Moro, 5, 00185 Roma, Italy, and
CNR Istituto di Geologia Ambientale e Geoingegneria (IGAG) c/o Dipartimento di Scienze della Terra, Università degli Studi di Roma La Sapienza, P.le A. Moro, 5, 00185 Roma, Italy

Don L. Anderson†
Seismological Laboratory, California Institute of Technology, MS 252-21, Pasadena, California 91125, USA

"Sunt aliquot quoque res quarum unam dicere causam / non satis est, verum pluris, unde una tamen sit" (There are phenomena for which it is not sufficient to infer a single origin, but it is necessary to propose several, among which, however, only one is true).
—Lucretius, De Rerum Natura (VI.703–704)

ABSTRACT

High-temperature geochemistry combined with igneous petrology is an essential tool to infer the conditions of magma generation and evolution in the Earth's interior. During the past thirty years, a large number of geochemical models of the Earth, essentially inferred from the isotopic composition of basaltic rocks, have been proposed. These geochemical models have paid little attention to basic physics concepts, broadband seismology, or geological evidence, with the effect of producing results that are constrained more by assumptions than by data or first principles. This may not be evident to seismologists and geodynamicists.

A common view in igneous petrology, seismology, and mantle modeling is that isotope geochemistry (e.g., the Rb-Sr, Sm-Nd, U-Th-Pb, U-Th-He, Re-Os, Lu-Hf, and other less commonly used systems) has the power to identify physical regions in the mantle, their depths, their rheological behavior, and the thermal conditions of magma generation. We demonstrate the fallacy of this approach and the model-dependent conclusions that emerge from unconstrained or poorly constrained geochemical models that do not consider physics, seismology (other than teleseismic travel-time tomography and particularly compelling colored mantle cross sections), and geology.

*Corresponding author; michele.lustrino@uniroma1.it
†Deceased

Lustrino, M., and Anderson, D.L., 2015, The mantle isotopic printer: Basic mantle plume geochemistry for seismologists and geodynamicists, *in* Foulger, G.R., Lustrino, M., and King, S.D., eds., The Interdisciplinary Earth: A Volume in Honor of Don L. Anderson: Geological Society of America Special Paper 514 and American Geophysical Union Special Publication 71, p. 257–279, doi:10.1130/2015.2514(16).

Our view may be compared with computer printers. These can reproduce the entire range of colors using a limited number of basic colors (black, magenta, yellow, and cyan). Similarly, the isotopic composition of oceanic basalts and nearly all their primitive continental counterparts can be expressed in terms of a few mantle end members. The four most important (actually "most extreme", because some are extraordinarily rare) mantle end members identified by isotope geochemists are DMM or DUM (depleted MORB [mid-ocean-ridge basalt] mantle or depleted upper mantle), HIMU (high mu, where mu = μ = $^{238}U/^{204}Pb$), EMI, and EMII (enriched mantle type I and type II). Other mantle end members, or components, have been proposed in the geochemical literature (e.g., PHeM, FOZO, LVC, PreMa, EMIII, CMR, LOMU, and C), but these can be considered to be less extreme components or mixtures in the geochemical mantle zoo.

Assuming the existence of these extreme "colors" in the mantle isotopic printer, the only matter for debate is their location in the Earth's interior. At least three of them need long-term insulation from convection-driven homogenization or mixing processes. In other words, where these extreme isotopic end members are located needs to be defined. In our view, no geochemical, geological, geophysical, or physical arguments require the derivation of any magma from deep mantle sources. Arguments to the contrary are assumption based. The HIMU, EMI, and EMII end members can be entirely located in the shallow non-convecting volume of the mantle, while the fourth, which is by far the more abundant volumetrically (DMM or DUM), can reside in the transition zone.

This view is inverted compared with current canonical geochemical views of the Earth's mantle, where the shallowest portions are assumed to be DMM like (ambient mantle) and the EMI-EMII-HIMU end members are assumed to be isolated, located in the deep mantle, and associated with thermal anomalies. We argue that the ancient, depleted signatures of DMM imply long-term isolation from recycling and crustal contamination while the enriched components are not free of contamination by shallow materials and can therefore be shallow.

INTRODUCTION

Despite nearly half a century of detailed study, a consensus on the thermal state and chemical composition of the Earth's interior has not yet been reached. The current canonical models of geochemistry evolved essentially independently of classical physics-, thermodynamics-, and seismology-based models. Secondary issues are not well resolved, and the gross features of the Earth are the subject of debate. Among these, the geothermal gradient of the deep Earth and the chemical versus thermal causes for absolute and relative changes in seismic wave speed with depth are debated (e.g., Anderson, 2007, 2011, 2013; Foulger et al., 2013). To constrain the basic features of the Earth's structure, it is essential to understand the dynamics of our planet in terms of petrogenetic processes.

The origin of igneous activity in intra-plate settings remains far from fully understood. At one time it was considered to be a solved problem. In one view, cracks and fractures tapped existing melts in the low-velocity zone under the fast-moving plates (the "jet-stream" of Wilson, 1963), but other views were that deep sources were required for the existence of island chains and that melts in the shallow mantle away from plate boundaries required deep, hot upwellings (e.g., Morgan, 1971, 1972). Recent high-resolution global marine gravity models of the oceanic basins reveal a wealth of buried tectonic structures, many of which may be of igneous origin (Sandwell et al., 2014). These features obscure the early defined oceanic chain trends, allowing the hypothesis of more widespread igneous activity, possibly related to the close-to-solidus condition of the shallow mantle.

While a general consensus has been reached on the causes of partial melting of the shallow mantle beneath oceanic ridges and along subduction zones, the origin of intra-plate igneous activity is still the subject of two different models based on opposite philosophical views.

Plume-Based Model

The first model argues that in order to have melts in areas away from plate boundaries, it is necessary to invoke thermal anomalies in the form of solid, deep mantle upwellings called mantle plumes. In this model, the buoyancy of mantle plumes is related to their derivation from the lowermost mantle (the seismic D″ region) and its superadiabatic gradient. Adiabaticity is related to relaxation as pressure decreases. The assumed adiabatic

gradient for solid mantle rocks is ~0.4–0.6 °C/km, while more compressible liquids are characterized by higher adiabatic gradients around 1 °C/km (McKenzie and Bickle, 1988; Anderson, 2007). A superadiabatic gradient refers to temperature decrease (with decreasing pressure) >0.6 °C/km. Superadiabatic gradients are necessary for convection.

The mantle plume model requires important assumptions: (1) a chemically homogeneous upper mantle characterized by a restitic (refractory) composition (harzburgitic to low-clinopyroxene lherzolitic) unable to produce large amounts of basaltic melts (e.g., Cadoux et al., 2007; Pfander et al., 2012; Hart, 2014); (2) a maximum temperature at the base of the seismic LID (the outermost shell of Earth characterized by an increase of seismic waves with depth) of ~1300 °C (e.g., McKenzie and Bickle, 1988; Fullea et al., 2009); (3) low-temperature and isothermal conditions for the entire sublithospheric mantle down to the transition zone (assumed in some mantle plume numerical modeling), the mantle volume extending between the olivine-wadsleyite polymorph transition at ~410 km and the ringwoodite-bridgmanite transition (the first is an olivine polymorph, while the second is Mg-Fe silicate perovskite) occurring at ~660–670 km (e.g., Sobolev et al., 2011); (4) the presence of a primitive (i.e., never before, or only poorly, melted or degassed) lower mantle resembling CI chondrites (i.e., the most primitive compositions in the solar system, represented by the carbonaceous chondrites type Ivuna); an alternative model relates the gas-rich D″ region to accumulation of noble gas–rich recycled hybrid pyroxenites and subducted eclogites (e.g., Davies, 2011); (5) an overall adiabatic geotherm for the bulk of the mantle (from ~250 to ~2800 km depth; e.g., Glisovic and Forte, 2014); (6) high "excess" potential temperatures (T_p) of plume mantle (hypothesized on the basis of geochemical arguments relating to magma compositions; Putirka 2005; Herzberg, 2011), where T_p is the temperature of a solid rock brought to the surface adiabatically, resulting in a decrease of ~0.4–0.6 °C/km; and (7) negative Vp and Vs seismic anomalies exclusively or mostly related to temperature excess (Montelli et al., 2004; White, 2010; Faccenna and Becker, 2010).

On these grounds, partial melting in the shallow intra-plate mantle is considered improbable (at least to high degrees) given that this volume is assumed to be too cold and too refractory. Consequentially, the source of intra-plate magma was considered to be related to solid mantle upwellings from depths as great as 2800–2900 km (e.g., Morgan, 1971, 1972; White, 2010; Li et al., 2014). The requirement of a single convection system involving the entire sublithospheric mantle is a conundrum in this model.

High T_p of mantle plumes cannot be directly measured and are assumed on the basis of the high forsterite (Fo) content [Fo = Mg/(Mg + Fe)] of olivines found in basaltic melts. Olivines are common minerals in equilibrium with high-temperature melts. During peridotite partial melting, Fe in olivines (and all other common silicate minerals present in the mantle: orthopyroxene, clinopyroxene, and garnet) is preferentially partitioned into the melt compared to Mg. At the same time, when olivine crystallizes in a cooling basaltic magma, it preferentially hosts Mg compared to Fe. This means that the maximum Fo content in an olivine crystallizing from a primitive basaltic melt (typically 0.75–0.85) is always lower than the Fo content in the peridotite (typically 0.90–0.93).

In order to have a Fo-rich olivine in a basaltic magma, a lot of Mg must be available in the crystallizing melt. According to the common view (e.g., Herzberg, 2011; Campbell and Griffiths, 2014), in order to have a lot of Mg in a basaltic melt, very high temperatures are required (because otherwise, MgO prefers to remain in the solid residua). The typical rationale is, then, that high-Fo olivine in a melt indicates high MgO in the crystallizing magma and, consequentially, this assumes high T to generate such magma, resulting in a high T_p estimate. As we show below, high-temperature regimes are only one of the possible ways to explain a high MgO content in a melt.

Shallow Earth Dynamics–Based Model

The second model considers the presence of chemical, and only minimally thermal anomalies to explain partial melting processes and seismic wave speed heterogeneities. Olivine-poor lithologies characterized by low solidus temperature can melt under "normal" conditions, without requiring a heat excess. In other words, in order to have partial melt production in the mantle, it is necessary to have high homologous temperature (the ratio of the mantle absolute temperature to the solidus temperature), not high absolute temperature (e.g., Anderson, 2007; Foulger, 2010). In this view, the upper mantle is completely different from that hypothesized in the previous model. It is a chemically, mineralogically, thermally, and rheologically heterogeneous mélange, a sort of a sheared baklava, marble-cake, or plum-pudding system. Here, volumetrically predominant olivine-rich lithologies (harzburgitic to lherzolitic matrix) are associated with olivine-poor to olivine-free, garnet + pyroxene ± phlogopite ± amphibole–rich lithologies, representing subducted lithologies, frozen basaltic melts, or the reaction products of melts derived from carbonated-hydrated subducted lithologies within the peridotitic matrix (e.g., Niu et al., 2011; Mallik and Dasgupta, 2014; Pilet, this volume).

Melts characterized by high bulk MgO content are commonly associated with high-MgO olivines, with Fo as high as 95%. A Fo content >95% means that 95 atoms out of 100, excluding Si and O and other minor bivalent constituents, are Mg, the remaining being Fe^{2+}. These high-MgO melts and minerals are found also in very low-volume continental Ca-Na-Al-Ti–poor ultrapotassic subduction-related rocks, which are certainly unrelated to mantle plumes (e.g., Prelevic and Foley, 2007). High MgO content in magma and associated olivine, coupled with low content of "basaltic" components (i.e., elements that typically partition into the melt during mantle anatexis), indicate that the source material was depleted (i.e., was involved in former partial melt extraction event[s]). This rules out any connection between the MgO content (in melt and olivine) and absolute temperature of formation, but rather associates MgO-rich melts and Fo-rich olivines with Fe-poor (depleted) mantle sources (e.g., Keiding et al., 2011).

Recent geophysical and petrological considerations (e.g., Kawakatsu et al., 2009; Anderson, 2011, 2013) have modified the shallow mantle model for intra-plate volcanism, hypothesizing the presence of diffuse melt lamellae in the low-velocity zone, a volume known from seismology since the 1960s (Gutenberg, 1959; Fig. 1B). Vp and Vs wave speeds are consistent with a ~100–150-km-thick layer at depths of 200 ± 50 km containing small melt pods. These melt lamellae, aligned in a peridotitic matrix, are assumed not to be in physical contact with each other and, therefore, cannot easily escape to the surface.

The solidus temperature of a natural system is the temperature at which the first melt drop is produced. Natural systems can experience partial melting if temperature increases. This is the basis on which the mantle plume theory rests (e.g., Putirka et al.,

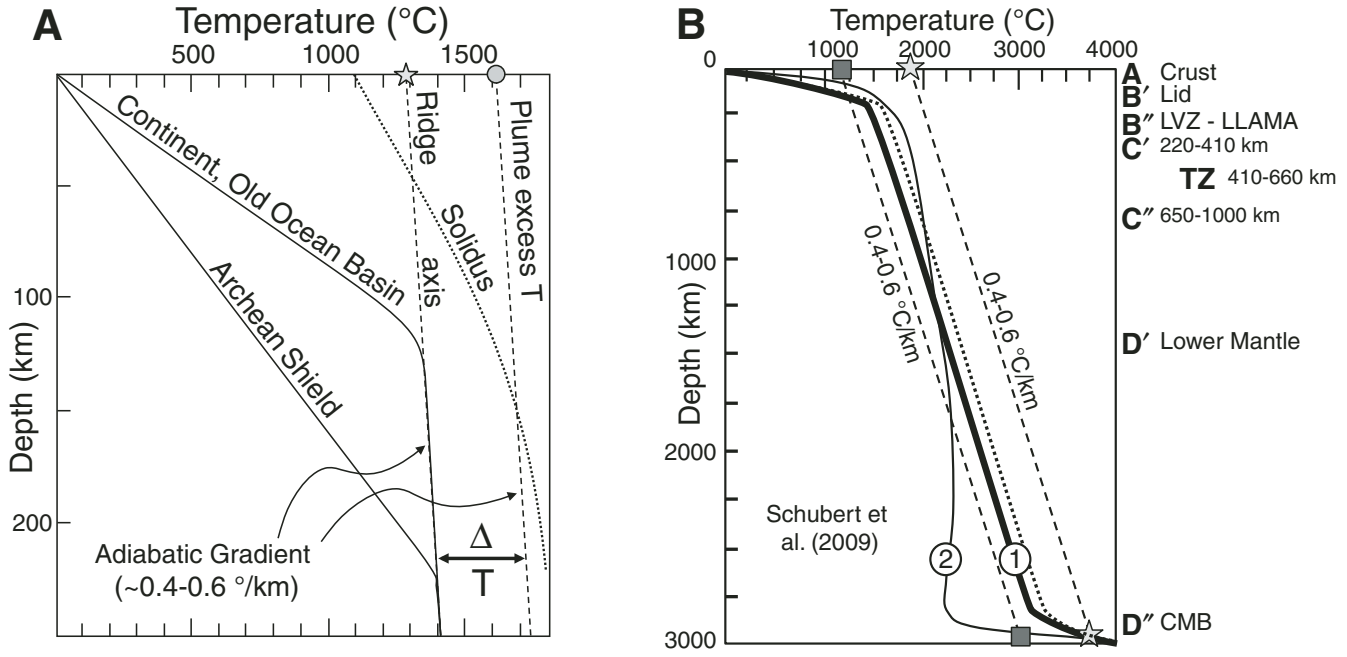

Figure 1. (A) Temperature–pressure (*T-P*) simplified scheme of the classical view of Earth's shallow interior (modified from McKenzie and Bickle, 1988). Two geotherms for Archean shield and old oceanic basin are shown. Dotted line indicates the solidus temperature (the temperature at which the first melt appears) for a pyrolite system. Pyrolite is an hypothetical chemical composition obtained by adding three parts by mass of depleted peridotite (dunite) and one part of tholeiitic basalt (Ringwood, 1979). To the left of the solidus, the temperature is too low for melting at any pressure. To the right of the solidus some melt is present. According to this geotherm, no melt should be present in the upper mantle. Dashed lines indicate the adiabatic gradient, i.e., the temperature decrease per kilometer of solid rock. ΔT indicates the heat excess of plume sources compared to "normal" convecting mantle. Mantle potential temperature (T_p) is a concept proposed by McKenzie and Bickle (1988) and corresponds to the temperature of magma or solid mantle if brought to the Earth's surface. According to McKenzie and Bickle (1988), mid-ocean-ridge basalt (MORB) T_p is slightly less than 1300 °C (star). The plume heat excess is measured by higher T_p (circle). (B) Temperature-pressure simplified scheme of Earth's mantle. The thick line (1) schematically represents the classically accepted geotherm with two thermal boundary layers characterized by superadiabatic regimes, one close to the surface and the other at the top of the core, with the bulk of the mantle characterized by an adiabatic geotherm. The thin line (2) is an alternative geotherm (Schubert et al., 2009) characterized by superadiabatic and subadiabatic geotherms and no adiabatic gradients. In the geotherm (1) the maximum *T* is reached at the base of the lithosphere (~90–100 km in oceanic basins), with T_p as high as ~1300 °C. Deeper mantle is hotter because it is self-compressed, but when brought to the Earth's surface (without melting) it is characterized by the same T_p (~1300 °C) as sublithospheric mantle. This temperature is considered to be ambient mantle T_p, and recorded by MORB (e.g., McKenzie and Bickle, 1988). Worth noting, more recent models hypothesize much hotter ambient mantle, with T_p in the order of 1440 °C (dotted line; Putirka et al., 2007). The most important differences between the two type of geotherms are: (a) the maximum T_p of geotherm (1) in the region B″ is lower than that of geotherm (2); (b) the maximum T_p of geotherm (1) in the shallow mantle is reached at shallower depths than the maximum T_p of geotherm (2); (c) after the thermal bump at ~200 km the T_p in geotherm (2) decreases with depth (following a subadiabatic gradient) while the T_p in geotherm (1) remains constant for nearly the entire mantle (following an adiabatic gradient, with the exception of the D″ region); and (d) region D″ in geotherm (1) is characterized by higher T_p than the entire mantle, while in geotherm (2) much of region D″ is characterized by lower T_p. The dashed lines represent the adiabatic upwelling of two samples of the lowermost mantle starting at temperatures compatible with geotherm (1) (star) and geotherm (2) (square). In the first case, which represents the classical mantle plume scheme, upwelling of solid mantle from D″ is characterized by higher T_p, recorded in high T_p magma (inferred on the basis of high Mg/Fe ratios). In the second case (the fluid-dynamically and internally heated compatible model) upwelling of solid mantle from D″ should be characterized by lower T_p. The highest T_p in geotherrn (2) region B″, corresponding to the LLAMA (layer of laterally advecting mantle anisotropy) mantle of Anderson (2011), around 200–250 km depth, corresponding to the worldwide, well-defined low-velocity zone (LVZ). A, B, C, and D on the right of the figure represent the original seismological zones into which the Earth was divided (modified from Anderson, 2011). CMB—core mantle boundary; TZ—transition zone mantle.

2007). A temperature excess is expected to be associated with upwelling of solid diapirs from the base of the lowermost mantle.

Alternatively, melts can be produced under "normal" conditions (i.e., without invoking absolute temperature excess) if H and/or C are available. Hydrogen can break the bonding oxygens connecting the SiO_4^{4-} tetrahedrons of mantle minerals and eventually lead to strong viscosity reduction and partial melting.

The maximum amount of H_2O that can be stored in pyroxenes, olivine, and garnet in the shallow mantle (i.e., at pressures <14 GPa, corresponding to ~410 km depth) does not exceed 0.1–0.2 wt%. Higher amounts of H_2O can be stored in the upper mantle in so-called "exotic" mantle silicates such as mica and amphibole, minerals that can host up to ~3 wt% H_2O. Rarely up to 10–12 wt% H_2O can be stored in other silicates such as antigorite, chlorite, and lawsonite (Schmidt and Poli, 2014; Vitale Brovarone and Beyssac, 2014). The presence of these minerals, however, is conditioned to the presence of light elements such as K (for the phlogopite mica) and Ca (for pargasite amphibole and lawsonite) and low temperature regimes in general. With increasing pressure, olivine polymorphs (wadsleyite and ringwoodite) become more prone to host water, and up to 2.5 wt% H_2O can be forced into their lattices (Pearson et al., 2014).

In contrast with hydrogen, carbon is a completely incompatible element in typical silicate mantle minerals. This means that, even at small levels, it forms its own solid phases (e.g., graphite, diamond, carbonates, iron carbides) or partitions into melts (e.g., Hirschmann and Dasgupta, 2009).

The water storage capacity of a mantle rock is the weighted sum of the maximum amount of H_2O that can be stored in the minerals. This capacity is variable and generally low—no more than 0.4–0.5 wt% at pressures <3 GPa, reducing to <0.1 wt% in the pressure range 3–14 GPa (Green et al., 2010). A water content below the maximum storage capacity means that no free water is available, all the H_2O being stored in silicate minerals. Under these circumstances the effect of the water in breaking the bonding oxygens is weak. Only if vapor-saturated conditions are reached (i.e., the amount of water exceeds the maximum water storage capacity of the mantle rocks) is partial melting encouraged, as the solidus temperature abruptly drops. The difference in solidus temperature between volatile-free and vapor-saturated conditions can be as much as 500 °C at 4 GPa (e.g., Litasov, 2011).

The most common hydrous phase in the mantle (pargasitic amphibole) is stable at depths shallower than ~100 km. The other hydrous phases (the so-called alphabet phases, synthesized in the laboratory only, like phases A, B, E, super E, 10 Å, and so on) are stable only at temperatures much lower than "normal" geotherms (e.g., Litasov and Ohtani, 2003; Schmidt and Poli, 2014).

The presence of stable carbonate minerals (essentially in the form of dolomite [$CaMg(CO_3)_2$] to magnesite [$MgCO_3$]) contributes to lowering the solidus temperature of the peridotitic assemblage, favoring melts with carbonatitic to carbonate-silicate compositions (e.g., Lee et al., 2000; Gudfinnsson and Presnall, 2005; Keshav and Gudfinnsson, 2014). This happens because the solidus temperature of carbonate minerals at mantle depths is several hundred degrees lower than for volatile-free silicate minerals (with a ΔT >500 °C at 4 GPa).

The presence of melt may thus be related not to absolute temperature excesses but to small amounts of CO_2 (easily prone to react with mantle silicates to produce Mg-Ca-Fe carbonates, minerals characterized by low melting temperature), high water contents (above the water storage capacity), or the absence of hydrous minerals at "normal" geotherm values. In other words, melting can be present in conditions of high homologous temperature.

HOW TO UNDERSTAND THE EARTH'S INTERIOR

Earth's Thermal Profile

As stated by White (2010, p. 134), "the plume hypothesis is essentially a physical one". Also Hofmann (2014) underlines that "most geochemical tracers carry no information about the specific mantle depth being sampled" and that "geochemistry cannot prove mantle plumes", meaning that the mantle plume concept is based on a hypothetical structural model of the Earth's interior, and that geochemistry is an ancillary discipline serving to strengthen the model. Foulger et al. (2013) highlighted the fundamental limitations of, and uncertainties in, seismic tomographic results. These uncertainties include the difficulty of defining background models and obtaining absolute seismic anomalies. These uncertainties derive from the variable chemical compositions and thermal states of the upper mantle. In order to translate into temperature a seismic wave speed anomaly, it is necessary to know the physical parameters of that volume (bulk and shear moduli, thermal expansion and compressibility parameters, anisotropy, presence of volatiles, melts, and exotic phases, Fe-Mg ratios in the main minerals, grain size, and so on). Only assuming *a priori* chemical, mineralogical, and lithological compositions may the tomographic results be interpreted in terms of mantle temperature. Clearly, these parameters cannot be known everywhere for heterogeneous systems like the upper mantle. Smith (this volume) underlines that when anisotropy is taken into consideration, the wave speed reductions interpreted as temperature anomalies in classical tomographic images (assuming isotropic mantle structure) simply disappear.

Fluid dynamic simulations of the Earth's interior and geochemical arguments on basaltic volcanism typically assume core temperatures maintained constant by the release of latent heat of crystallization of the liquid core (e.g., Schuberth et al., 2009; Campbell and Griffiths, 2014; Nakagawa and Tackley, 2014).

The classical seismological scheme of Earth's interior involves four main regions (regions B, C, and D; Fig. 1B), with the crust representing region A. The uppermost ~200 km of the Earth (regions A and B) is characterized by a superadiabatic gradient, with rapid temperature increase over a relatively small depth range, passing from temperatures near zero to ~1300–1500 °C at its base (Fig. 1).

The lower part of region B (known as B″) is a thermal and shear boundary layer. The bulk of the mantle (all but region B) is usually assumed to be adiabatic down to the core-mantle boundary layer at ~2700–2800 km. This cannot be the case for an internally heated or secularly cooling mantle. The base of the lowermost mantle, region D″, is characterized by another sharp increase of temperature (superadiabatic gradient) estimated between 800 and 1300 °C (Jeanloz and Morris, 1986; Boehler et al., 1995; Campbell and Griffiths, 2014; Fig. 1B).

According to this classical view, the two most important thermal boundary layers of the Earth's interior are the very shallow regions (which contain the lithosphere, LID, and plate—regions A and B′; see Anderson [2011] for a review of the different meanings and implications of these terms) and region D″ located at ~2800–2900 km depth. To resume, the canonical view assumes an adiabatic geotherm for the bulk of the mantle, a superadiabatic D″ (caused by the strong heating from below), a vigorous whole-mantle convection below region B′, a consequent chemical homogeneity, lack of layering, no internal heating, and no slabs to cool its interior (Figs. 1A and 1B). The T_p of the adiabatic interior of the Earth is assumed ranging from 1280 °C to 1500 °C, with mantle plume–influenced regions being characterized by temperature excess ranging from 100 °C to 400 °C (McKenzie and Bickle, 1988; Putirka et al., 2007; White, 2010; Campbell and Griffiths, 2014). According to this pot-on-the-stove view, the Earth's mantle is heated from below by a constant-temperature heat source.

A corollary of fluid dynamic simulations is a self-compressed Earth heated by a constant-temperature core-mantle boundary triggering whole-mantle overturn, with limited obstruction, if any, by the transition zone. Hot, solid, but narrow mantle blobs are assumed to depart from the D″ layer, moving through the entire mantle, and eventually melting when they reach relatively shallow mantle depths (Fig. 1B). Both early and recent modeling (e.g., Griffiths and Campbell, 1990; Farnetani and Richards, 1994; Ballmer et al., 2013; Cloetingh et al., 2013; Bull et al., 2014; Li et al., 2014) assume prescribed and constant temperatures, modes of convection, adiabaticity, and non-cooling interfaces.

Alternatively, mantle convection could be caused by heat lost from the surface to space rather than by heat released by the crystallizing liquid core. The differences are not subtle. In the former case, surface cooling triggers convection, favoring delamination of cold portions of the shallow mantle and passive upwelling in the mantle (e.g., Anderson and King, 2014; Anderson and Natland, 2014). Moreover, the mantle cools the core, while in plume modeling and in canonical geodynamic and geochemical models, the core warms the mantle and convection is caused by heat excess at D″.

The thick line indicated with "1" in Figure 1B represents schematically the classically accepted geotherm with two thermal boundary layers characterized by superadiabatic regimes, one close to the surface (regions A and B′) and the other on top of the core (region D″), with the bulk of the mantle characterized by an adiabatic geotherm (regions B″, C, and D′). The thin line indicated with "2" in the same figure is one of the possible geotherms (Schubert et al., 2009) characterized by superadiabatic and subadiabatic trends and no adiabatic gradients. In the first scheme, with the exclusion of D″, maximum T_p is reached at the base of the lithosphere (~90–100 km in oceanic basins), with T_p as high as ~1300 °C. Deeper mantle is hotter because it is self-compressed, but when brought to a reference pressure (e.g., the Earth's surface) it is characterized by the same T_p (~1300 °C) as the sublithospheric mantle. This temperature is considered the ambient mantle T_p, as recorded by mid-ocean-ridge basalt (MORB; e.g., McKenzie and Bickle, 1988). More recent T_p estimates of the ambient mantle T_p reach values as high as 1440 °C (Putirka et al., 2007) or 1500 °C (Presnall and Gudfinnsson, 2011). In this case, however, the hypothesized heat excess of plume sources compared with ambient mantle remains the same (i.e., both the ambient mantle and the plume mantle are hotter than the original estimates of McKenzie and Bickle, 1988). The most important differences between the two type of geotherms are: (1) the maximum T_p of geotherm 1 is lower than that of geotherm 2; (2) the maximum T_p of geotherm 1 is reached at shallower depths than geotherm 2; (3) after the thermal bump at ~200 km the T_p in geotherm 2 decreases with depth while the T_p in geotherm 1 remains constant for nearly the entire mantle; and (4) D″ in geotherm 1 is characterized by higher T_p than the entire mantle, while in geotherm 2 much of D″ is characterized by lower T_p.

The dashed lines in Figure 1B represent the adiabatic upwelling of two samples of the lowermost mantle starting at temperatures compatible with geotherm 1 (star) and geotherm 2 (square). In the first case (the classical mantle plume scheme) upwelling of solid mantle from D″ is characterized by higher T_p, recorded in high-T_p magma (inferred on the basis of high Mg/Fe ratios of melts and associated olivines). In the second case (the fluid dynamically and internally heated compatible model) upwelling of solid mantle from D″ is characterized by lower T_p. The highest measurable T_p in this case is associated with mantle corresponding to the LLAMA (laminated lithology with aligned melt accumulations, or layer of laterally advecting mass and anisotropy) region of Anderson (2011), around 200–250 km depth, corresponding to the worldwide, well-defined low-velocity zone (LVZ). What emerges is the (apparent) paradox that the deeper the source the colder the T_p. The importance of this region (also corresponding to the old "perisphere" of Anderson [1995]) has been recently emphasized by Smith (this volume).

Can Geochemistry Help?

The reason why plumes are still part of the canonical models of mantle geochemistry and dynamics can be traced to insufficient interdisciplinary understanding, unquestioning acceptance of the conclusions of others, and semantics. This is known in philosophy as incommensurability. Seismologists are generally not fully aware of the assumptions underlying geochemical inferences and simply accept the conclusions regarding primordial and undegassed mantles and the meaning of concepts such as

high $^{3}He/^{4}He$ or given Pb isotopic ratios. Likewise, geochemists are generally not completely aware of the modeling assumptions in teleseismic travel-time tomography and tend to interpret color images of the mantle as thermometry. High-resolution seismic tomography has confirmed that the mantle features used as evidence for active plumes are thousands of kilometers in lateral extent and therefore probably neutral, passive, and rising only slowly if at all. As a consequence, an alternative view (i.e., that they are not thermal plumes or active upwellings) has been proposed (e.g., Anderson and Natland, 2014). It has also been confirmed that intra-plate volcanoes such as Hawaii tap into a thick sheared shallow boundary layer that is sufficiently hot, fertile, large, and slowly moving to explain volcanic chains (Anderson, 2011; Smith, this volume). Surprisingly, this was the original conclusion proposed by Wilson (1963). This shallow layer is disrupted by three-dimensional deep passive upwellings that feed ridges and near-ridge hotspots.

The canonical paradigm of mantle dynamics and geochemistry includes whole-mantle convection and whole-mantle plumes. It has been supported by three lines of evidence: radiogenic isotope geochemistry, fluid dynamic simulations, and relative travel-time tomography. Each of these has undergone paradigm shifts, even reversals, requiring reconsideration of the whole canonical model. In the next sections we focus on those isotopic systematics most widely used in basalt petrogenesis. We demonstrate how geochemical concepts do not require deep mantle upwelling and, consequentially, cannot be used as "smoking guns" for mantle plumes. Statements such as "the *X* value of the *Y* isotopic systematic indicates the involvement of deep mantle plumes" are simply incorrect. Geochemistry does not have the power to detect upwellings from the deep mantle and has only limited power to infer the thermal state of the melt source.

PRINCIPLES OF GEOCHEMISTRY APPLIED TO IGNEOUS PETROLOGY

The upper thermal boundary layer, the upper 150–200 km of the Earth, is physically and geochemically heterogeneous. This is confirmed by the mineralogy and geochemistry of the alkali basalt borne xenoliths representative of the 50–120 km depth range of the mantle (Nixon, 1987).

Despite this, the upper mantle is commonly assumed to be homogeneous, isotropic, chemically depleted, olivine-rich, and nearly H and C free by geochemists and geophysical modelers (e.g., Cadoux et al., 2007). In particular, the shallowest rigid portion of the mantle is considered to be stiff and virtually incapable of producing basaltic melts unless at unrealistically high temperatures. Sometimes the lithosphere is equated to the seismic LID or to the whole boundary layer. These background hypotheses have important implications for interpreting isotopic "anomalies" in mantle-derived materials and the travel-time anomalies of teleseismic waves. The LID and the lithosphere are thin, and this is one reason why geochemists look much deeper for magma sources.

In the standard geochemical model, the deep mantle is not involved in chemical differentiation. It maintained a primordial chemical composition despite being continuously modified (enriched in basaltic components) by arrival of subducted material that pierced the transition zone. Several geochemical models, based on unconstrained assumptions and forcing a selected set of data to converge toward pre-fixed results, attempt to explain this paradox (e.g., Jackson et al., 2010, 2014; Davies, 2011).

Standard geochemical models require background lower-mantle or liquid-core thermal and chemical inputs to explain the genesis of ocean-island basalt (OIB) and other supposed plume-related volcanism. In geochemistry, OIB is a generic term for intra-plate oceanic rocks characterized by a large range of incompatible element contents and a very large range of isotopic ratios. This rock group comprises volumetrically predominant tholeiitic (i.e., Na-K poor and with relatively high Fe/Mg) and minor sodic alkaline basalts, along with very rare differentiated (i.e., silica-richer) compositions such as trachytes and phonolites. In isotope geochemistry, the term OIB is too vague and several prefixes (e.g., HIMU, EMI, EMII, and so on, which we explain later) are needed to distinguish the various compositions.

In particular, isotope geochemistry is often considered by geochemists and geophysicists to be the smoking gun for mantle plumes. We explain here why isotope geochemistry cannot be used as evidence, much less definitive proof, for mantle plumes.

The Rb-Sr Isotope System

This is the oldest and best-studied isotopic system applied to igneous petrogenesis (e.g., Faure and Powell, 1972). It is based on the natural decay (i.e., transformation) of a radioactive isotope of rubidium, ^{87}Rb (representing ~27.8% of the isotopes of Rb, the remaining being the stable ^{85}Rb). Strontium has four stable isotopes, with atomic masses 84 (0.6% of the Sr isotopes), 86 (9.9%), 87 (7%), and 88 (82.6%). The abundance ratios among the Sr isotopes remain constant, with the exception of ^{87}Sr, which is continuously produced by ^{87}Rb decay.

The half-life of ^{87}Rb is 4.8×10^{10} yr (Table 1). Given that the age of the Earth is one-tenth of this half-life, clearly the original ^{87}Rb at the time of the Earth's formation has been reduced by only a small amount, and the amount of ^{87}Sr has increased by only the same amount. The amount of ^{87}Sr now measured in a rock (sedimentary, metamorphic, or igneous) is the sum of the original ^{87}Sr plus the amount produced after the decay of ^{87}Rb. Obviously, the higher the original content of Rb (and hence ^{87}Rb) and the older a rock, the larger the amount of radiogenic ^{87}Sr produced.

During partial melting or fractional crystallization processes, the most important differentiation processes in igneous geochemistry (except for the noble gases and stable isotopes), two isotopes of the same element (e.g., ^{88}Rb and ^{87}Rb, or ^{87}Sr and ^{86}Sr) are not fractionated and their ratios remain unchanged. What may change is the elemental ratio of the parent and daughter isotope pairs. The ionic radius of Rb (1.66 Å, where

TABLE 1. MAIN PARENT-DAUGHTER ISOTOPIC CHARACTERISTICS OF THE SYSTEMATICS DISCUSSED IN THE TEXT

Parent	%	Half-life	Daughter	Parent/daughter ratios	Present day	Isotopic ratios	Initial	Present day
^{87}Rb	27.8	4.8×10^{10} yr	^{87}Sr	^{87}Rb/^{87}Sr	~0.072	^{87}Sr/^{86}Sr	0.69897	0.70445
^{147}Sm	15.0	1.06×10^{11} yr	^{143}Nd	^{147}Sm/^{143}Nd	~0.202	^{143}Nd/^{144}Nd	0.506687	0.51264
^{232}Th	100	1.4×10^{10} yr	^{208}Pb	^{232}Th/^{208}Pb	~36	^{206}Pb/^{204}Pb	9.31	N.A.
^{235}U	0.72	7.07×10^{8} yr	^{207}Pb	^{235}U/^{207}Pb	~8.5	^{207}Pb/^{204}Pb	10.29	N.A.
^{238}U	99.28	4.47×10^{9} yr	^{208}Pb	^{238}U/^{206}Pb	~0.06	^{208}Pb/^{204}Pb	29.48	N.A.

Note: The column "%" reports the mass abundance of that isotope compared to the remaining isotopic masses. N.A.—not applicable.

Å = angstrom = 1×10^{-10} m = 0.1 nm) is not much different from that of K (1.52 Å). Also the charge of Rb and K is the same (+1). These two characteristics render Rb an element with a geochemical behavior very similar to that of K. In other words, Rb can substitute or replace K in minerals (e.g., K-feldspars or biotite). On the other hand, Sr (1.32 Å; +2 valence) shares much more geochemical affinity with Ca (1.14 Å; +2 valence). The Earth's mantle has more Ca than K (Ca/K ratio of primitive mantle estimated to be ~75; Lyubetskaya and Korenaga, 2007).

During partial melting of a volatile-free peridotitic source, K behaves as a strongly incompatible element (i.e., it has a strong tendency to prefer the melt phase), because there are no minerals in which it can exist. Element incompatibility must always be expressed with respect to a given mineral (or mineral assemblage) and a given melt composition. The compatibility of an element is the ratio of its abundance in the mineral to its abundance in the liquid that is in equilibrium with it. There is no element that is always "incompatible" (i.e., prefers the liquid phase) or "compatible" (i.e., prefers the solid phase) under all conditions (e.g., Fedele et al., 2015).

Rubidium is incompatible in a peridotitic mantle. This means that, in the presence of melt, Rb is preferentially partitioned there instead of remaining in the solid rock residuum. The same Rb is compatible in a crystallizing rhyolitic melt (an alkali feldspar–rich volcanic rock). This means that Rb will preferentially move into the crystallizing alkali feldspar (or biotite) as it precipitates.

Calcium behaves as a moderately incompatible element (because the only mineral in which it can be stored, clinopyroxene, is among the first phases to melt). In a carbonated peridotite, Ca continues to behave as a moderately incompatible element, because carbonates are the first phases to melt due to their very low melting temperature compared with the other silicate minerals. The same holds in the presence of garnet, a phase that can host large amounts of Ca at large depth in its Ca-majoritic form, but which is among the first phases to melt. As a consequence, the K/Ca ratio (and also Rb/Sr) in a partial melt of a peridotite (e.g., basalt) is higher than the K/Ca (or Rb/Sr) in the source. The higher Rb/Sr, the higher ^{87}Rb/^{86}Sr, where the numerator is a radioactive nuclide and the denominator is a stable primordial isotope of Sr. With time, the higher ^{87}Rb/^{86}Sr evolves into higher ^{87}Sr/^{86}Sr because ^{87}Rb slowly transforms to ^{87}Sr, while the ^{86}Sr content does not change.

The present-day ^{87}Sr/^{86}Sr isotopic ratio of the bulk silicate Earth (BSE, which represents the solid Earth, excluding the core) is now known to be around 0.70445. This is the ratio the entire Earth should have, assuming an original undifferentiated Earth ^{87}Rb/^{86}Sr ratio (~0.09, present-day value) and an initial ^{87}Sr/^{86}Sr of 0.69897 (Fig. 2). The initial ^{87}Sr/^{86}Sr of the Earth, called BABI (basaltic achondrite best initial; Papanastassiou and Wasserburg, 1969), is the Sr isotopic ratio of a basaltic achondrite meteorite with no Rb (and thus no ^{87}Rb). This means that all of the ^{87}Sr in that meteorite represents the primordial ^{87}Sr content of the solar system. In other words, during its 4.56 b.y. life, the Earth's ^{87}Sr/^{86}Sr ratio has increased from 0.69897 (BABI) to 0.70445 (BSE), i.e., by only 0.00548, as result of ^{87}Rb decay. Modern thermal ionization mass spectrometers can easily measure these very small ratio differences, with the typical precision of ^{87}Sr/^{86}Sr ratios being $\pm 5 \times 10^{-6}$.

The present-day BSE value assumes an unchanged Rb/Sr isotopic ratio (Fig. 2). This is true if we assume the entire Earth as a single system. But what happens if we consider the basalt-restite mantle pair? (Restite is the residuum after extraction of partial melt.) Basalts are characterized by Rb/Sr ratios higher than the original mantle and the restitic mantle. As a consequence, with aging we should expect in the basalt higher ^{87}Sr/^{86}Sr, while the restitic mantle should be characterized by lower ^{87}Sr/^{86}Sr.

But how can the ^{87}Sr/^{86}Sr ratios in igneous rocks be used to constrain their origin? Let us assume that at a given moment (e.g., 2 b.y. after its formation), the Earth experiences partial melting (Fig. 2; first partial melting event). This is a differentiation process, producing a partial melt which eventually will solidify forming an igneous rock, leaving a restitic mantle. The first rock is characterized by higher Rb/Sr, while the second shows lower Rb/Sr. After ~2.5 b.y., the rock with higher Rb/Sr (and thus higher ^{87}Rb/^{86}Sr) will be characterized by a higher ^{87}Sr/^{86}Sr ratio compared with the restitic source (Fig. 2). Both sources will have ^{87}Sr/^{86}Sr higher than at the moment of partial melting, but the ^{87}Sr/^{86}Sr ratio of the igneous rock will be much higher than that of the restite. The ^{87}Sr/^{86}Sr ratio of the restite is characterized by a ^{87}Sr/^{86}Sr ratio lower than the present-day BSE ^{87}Sr/^{86}Sr. The solidified partial melt can experience partial melting itself (second partial melting event in Fig. 2). In this case, this process produces a new partial melt with higher Rb/Sr and a residual source with lower Rb/Sr that will evolve toward different ^{87}Sr/^{86}Sr ratios (Fig. 2).

A second partial melting event of the first mantle residuum (third partial melting event in Fig. 2) will produce a new melt and an even more depleted residuum. The final isotopic ratios

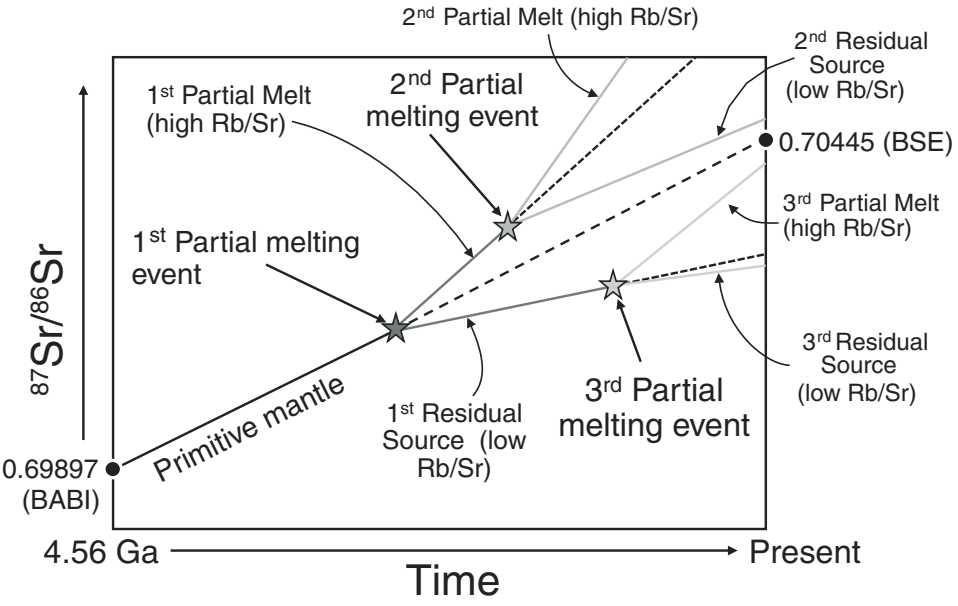

Figure 2. Schematic evolution of the $^{87}Sr/^{86}Sr$ isotopic ratio with time. ^{87}Sr is continuously produced by ^{87}Rb decay, while ^{86}Sr is the stable strontium isotope. As a consequence, $^{87}Sr/^{86}Sr$ continuously increases with time. Partial melting has the effect of increasing the isotopic ratio rate in the melt and reducing it in the solid residuum. BABI—basaltic achondrite best initial; BSE—bulk silicate Earth.

of the different partial melts and melt residua will depend on the initial $^{87}Sr/^{86}Sr$ ratios, the age of melt extraction, the degree of Rb/Sr fractionation (essentially a function of source mineralogy and degree of melting), and the ^{87}Rb half-life (Gast, 1960). In other words, a basalt (but also any other kind of igneous rock) characterized by $^{87}Sr/^{86}Sr$ ratio lower than that of BSE is considered derived from a depleted (i.e., non-primitive) mantle source. At a very large degree of melting, the liquid will have Rb/Sr ratios converging to the original (primordial) values. Such large degrees of melting occurred only during the accretion of the Earth.

What should the present day $^{87}Sr/^{86}Sr$ ratio of a basalt derived from a primitive mantle be (i.e., the composition assumed for the lower mantle in some models)? Such a rock should have an $^{87}Sr/^{86}Sr$ ratio similar or very close to the BSE estimate. A conundrum for the classical mantle plume model is that nearly all rocks whose origin is postulated to be related to plumes (e.g., HIMU OIB) are characterized by $^{87}Sr/^{86}Sr$ ratios lower than that of BSE, implying non-primitive mantle source compositions and former partial melt extraction. Only a few OIB (EMI and EMII types) are characterized by $^{87}Sr/^{86}Sr$ ratios higher than that of BSE, but essentially none has the same isotopic composition as BSE (Stracke, 2012).

Igneous rocks are not all confined to $^{87}Sr/^{86}Sr$ ratios less than that of BSE. An important part of the Earth (essentially the upper crust) is characterized by sedimentary, metamorphic, and igneous rocks with $^{87}Sr/^{86}Sr$ ratios higher than that of BSE. This results from faster radiogenic growth of ^{87}Sr in rocks with $^{87}Rb/^{86}Sr$ ratios higher than the primordial Earth value. The average upper crust (as represented by the global subducting sediment compilation of Plank [2014]) is old and characterized by high Rb (84 ppm; compare this value with 0.46 ppm Rb of the primitive mantle) and high Rb/Sr (0.27, compared this ratio with the 0.03 value of the primitive mantle), resulting in strongly radiogenic $^{87}Sr/^{86}Sr$ (0.7124; Plank, 2014).

Subduction is a process during which upper crust lithologies (or alteration products of them) are recycled back to the mantle. During this process, rocks with high $^{87}Sr/^{86}Sr$ ratios are again mixed with an upper mantle matrix characterized by $^{87}Sr/^{86}Sr$ ratios less than that of BSE. If such a crust-contaminated mantle experiences a new partial melting process, it is possible to obtain melts with a wide range of isotopic compositions, with values lower to much higher than the BSE estimate.

In conclusion, the $^{87}Sr/^{86}Sr$ ratios of igneous rocks can be used to constrain the depleted (low $^{87}Sr/^{86}Sr$, indicating long-term evolution of a low-Rb/Sr system, indicating old melt extraction, with Rb more incompatible than Sr) or the enriched (high $^{87}Sr/^{86}Sr$, indicating high Rb/Sr) character of their sources. This can be done quantitatively only if the age of the melt extraction events, their number, the amount of the melt extracted (the Rb/Sr of the melt varying as function of the degree of melting), the age of the recycling process during subduction, the isotopic and elemental composition of the original crustal material entering the trench, the metamorphic reactions in the subducting slab (able to fractionate Rb from Sr), and the style of interaction between fluids and/or melts released from the slab with the supra-subduction mantle wedge are precisely known. This is never the case. These factors can only be estimated, guessed, or assumed, and as a consequence, the results of a geochemical modeling always are only qualitative or semiquantitative at best.

Partial melting decreases the $^{87}Rb/^{86}Sr$ ratios of the mantle residuum, ultimately resulting in $^{87}Sr/^{86}Sr$ ratios lower than that of BSE. Recycling of upper crustal lithologies increases $^{87}Rb/^{86}Sr$ and the $^{87}Sr/^{86}Sr$ ratio of the supra-subduction mantle wedge, forcing it to higher $^{87}Sr/^{86}Sr$ ratios and toward values greater than that of BSE. What is clear is that the $^{87}Sr/^{86}Sr$

isotopic composition of an igneous rock whose $^{87}Sr/^{86}Sr$ ratio is lower than that of BSE clearly indicates derivation from a mantle source that has experienced partial melt extraction in its past, and $^{87}Sr/^{86}Sr$ ratios higher than that of BSE indicate derivation from a mantle that is not primitive.

Despite these simple considerations, $^{87}Sr/^{86}Sr$ ratios in basalts as low as 0.7025 are considered to reflect derivation from enriched end members classically identified with deep mantle upwelling in the form of mantle plumes (e.g., Merle et al., 2009). Ironically, such low $^{87}Sr/^{86}Sr$ values (coupled with high $^{143}Nd/^{144}Nd$ ratios, see below) were originally regarded as evidence of derivation from a depleted MORB-like source (e.g., Gast, 1968). The efforts to reconcile such kinds of evidence (depleted isotopic compositions) with a deep mantle source characterized by heat excess results in paradoxical models. Mantle plume sources made up by low-density refractory harzburgite matrix mixed with depleted recycled oceanic basalts (i.e., with no primitive compositions at all or only with a minor primitive/undegassed component) emerge indeed from thermodynamic, geochemical, and geophysical constraints (Jackson et al., 2014; Shorttle et al., 2014).

The Sm-Nd Isotope System

Samarium and neodymium belong to the rare earth element (REE) group, a suite of 14 incompatible elements all with the same charge with atomic number (Z) increasing from La ($Z = 57$) to Lu ($Z = 71$). The ionic radius of the REEs decreases slightly from La (1.17 Å) to Lu (1.00 Å). The same +3 valence of Nd ($Z = 60$) and Sm ($Z = 62$), but the slightly lower ionic radius of the latter (1.12 Å versus 1.10 Å for Nd and Sm, respectively), render Nd slightly more incompatible than Sm during mantle partial melting and basaltic melt crystallization (Fig. 3). Samarium is present in seven different isotopes, with atomic masses of 144 (3.1%), 147 (15%), 148 (11.2%), 149 (13.8%), 150 (7.4%), 152 (26.7%), and 154 (22.7%), of which only ^{147}Sm and ^{148}Sm are radioactive.

The half-life of ^{148}Sm is very long (7×10^{15} yr), and consequentially it can be considered to be a stable element on the time scale of the Earth. On the other hand, the half-life of ^{147}Sm is shorter (1.06×10^{11} yr), and its decay chain is relevant to geology. ^{147}Sm is transformed by α-decay into ^{143}Nd, and the ^{147}Sm-^{143}Nd system works in the same way as the ^{87}Rb-^{87}Sr system discussed above (Table 1). Given the longer half-life of ^{147}Sm (106 b.y.) compared to that of ^{87}Rb (48 b.y.), less ^{143}Nd than ^{87}Sr has been produced during Earth's lifetime. In absolute terms, however, the number of radiogenic ^{143}Nd atoms (15% of all the Nd isotopes) produced in 4.56 b.y. is higher than the number of radiogenic ^{87}Sr atoms because of the higher amount of ^{147}Sm compared with ^{87}Rb (7% of all the Rb isotopes). The only substantial difference from the Rb-Sr system is that the radioactive (parent) isotope (^{147}Sm) is less incompatible than the radiogenic (daughter) isotope ^{143}Nd. The definition "less incompatible" is here preferred to "more compatible" to highlight the general incompatible character of both Sm and Nd during peridotite partial melting.

Also in this case the radiogenic ^{143}Nd isotope is measured against a stable Nd isotope (^{144}Nd) according to the classical relation $^{143}Nd/^{144}Nd$. The Earth's primordial $^{143}Nd/^{144}Nd$ isotopic ratio is assumed to be the same as that of chondritic meteorites and is constrained to 0.512638 (defined as that of the chondritic uniform reservoir, CHUR), while $^{143}Nd/^{144}Nd$ at the time of formation of the solar system was 0.50669. In other words, $^{143}Nd/^{144}Nd$ during the last 4.56 b.y. has increased by 0.00595.

Several attempts have been made to modify the accepted concept of chondritic Earth to solve the problem raised by another Nd isotope (^{142}Nd), suggesting for the whole Earth a $^{143}Nd/^{144}Nd$ isotopic ratio more radiogenic than for CHUR (0.5130; Caro and Bourdon, 2010; Jackson and Jellinek, 2013). It is worth noting, however, that any modification of the accepted chondritic Earth assumption raises a large number of additional problems (e.g., for a super-chondritic $^{143}Nd/^{144}Nd$ value for the Earth, the depleted major- and trace-element content of MORB would be at odds with their "new" primitive Nd isotopic composition). As a consequence, we continue using the classically accepted chondritic (CHUR) value.

Neodymium is slightly more incompatible than samarium during partial melting, so a restitic mantle is characterized by lower Nd/Sm (and hence higher $^{147}Sm/^{144}Nd$) than the pre-melting composition and the basaltic melt. A rock with high $^{147}Sm/^{144}Nd$ will evolve, with aging, to high $^{143}Nd/^{144}Nd$ isotopic ratios (Fig. 3).

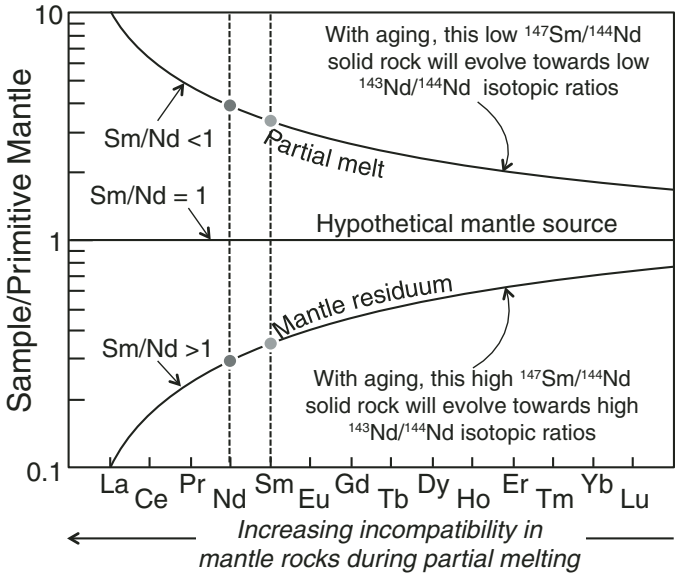

Figure 3. Rare earth elements normalized to primitive mantle estimates. The two curved lines indicate simplified patterns of partial melts and mantle solid residua after anatexis. The incompatibility of an element is its tendency to partition into the melt phase. Partial melts of a primitive mantle source are characterized by relatively low Sm/Nd ratios, while mantle residua are characterized by high Sm/Nd. With aging these elemental ratios will evolve toward low $^{143}Nd/^{144}Nd$ and high $^{143}Nd/^{144}Nd$, respectively.

Following the rationale described for the Rb-Sr isotopic system, an anciently depleted mantle source will be characterized by $^{143}Nd/^{144}Nd$ higher than that of CHUR and much higher than that of solidified partial melt (characterized by lower Sm/Nd, i.e., lower ^{147}Sm, and consequentially lower ^{143}Nd produced for a given amount of stable ^{144}Nd). Also in this case, igneous rocks interpreted as the products of mantle plumes tapping primitive mantle sources should be characterized by $^{143}Nd/^{144}Nd$ ratios very close to that of CHUR. However, they are nearly constantly shifted toward isotopically depleted (i.e., $^{143}Nd/^{144}Nd$ greater than that of CHUR) compositions, ruling out the existence of such primitive mantle compositions.

The Sr-Nd isotopic pair is at the base of isotope geochemistry applied to igneous petrology. All basaltic compositions erupted in oceanic or continental intra-plate settings plot along a trend, defined originally as the mantle array (e.g., DePaolo and Johnson, 1979; Figs. 4, 5A). This connects the isotopically depleted field (characterized by $^{87}Sr/^{86}Sr$ lower than that of BSE and $^{143}Nd/^{144}Nd$ higher than that of CHUR) with the isotopically enriched field ($^{87}Sr/^{86}Sr$ higher than that of BSE and $^{143}Nd/^{144}Nd$ lower than that of CHUR), passing through BSE-CHUR values (Fig. 4). MORB plot entirely in the depleted field, HIMU OIB plot nearly entirely in the depleted isotopic field, while EMI- and EMII-OIB extend to the enriched field (Fig. 5A).

In Figure 5A, a recent compilation of oceanic basalt isotopic data (Stracke, 2012) is plotted together with the four basic "colors" of the mantle isotopic printer. The DMM-HIMU-EMI-EMII irregular quadrilateral envelops >99% of oceanic basalts. As a consequence, their Sr-Nd isotopic composition can be simply explained in terms of the relative contribution of these four extreme values. This is the basis of isotope geochemistry applied to the petrogenesis of oceanic (and also continental, Fig. 5B) igneous rocks. Up to this point there is no fundamental disagreement between the geochemical and petrological communities except for the precise position of the four end members in Sr-Nd-Pb isotopic space. Problems emerge when trying to translate into geological terms these four end members, assigning thermal, rheological, physical, depth, and mineralogical meaning to these "colors".

The U-Th-Pb Isotope System

The uranium-thorium-lead system is more complex than the Rb-Sr and Sm-Nd systems. Here there are three radiogenic isotopes (^{238}U, ^{235}U, and ^{232}Th) that decay into three different radiogenic Pb isotopes (^{206}Pb, ^{207}Pb, and ^{208}Pb, respectively), with different half-lives and energy emissions. Uranium is present as two radioactive isotopes, with atomic masses 235 (0.72%) and 238 (99.28%). Thorium is present only as ^{232}Th, while Pb is present as four stable isotopes with masses 204 (1.4%), 206 (24.1%), 207 (22.1%), and 208 (52.4%).

As discussed previously, the ^{206}Pb, ^{207}Pb, and ^{208}Pb abundances slowly but continuously increase due to the decay of ^{238}U (half-life = 4.5 b.y.), ^{235}U (half-life = 0.7 b.y.), and ^{232}Th (half-life = 14.0 b.y.). In this case the three radiogenic Pb isotopes are normalized to ^{204}Pb. As a consequence, the U-Th-Pb isotopic system is conventionally reported as three separate isotopic ratios: $^{206}Pb/^{204}Pb$, $^{207}Pb/^{204}Pb$, and $^{208}Pb/^{204}Pb$. The $^{238}U/^{204}Pb$ isotopic ratio is defined as μ (mu), while $^{232}Th/^{238}U$ is defined as κ

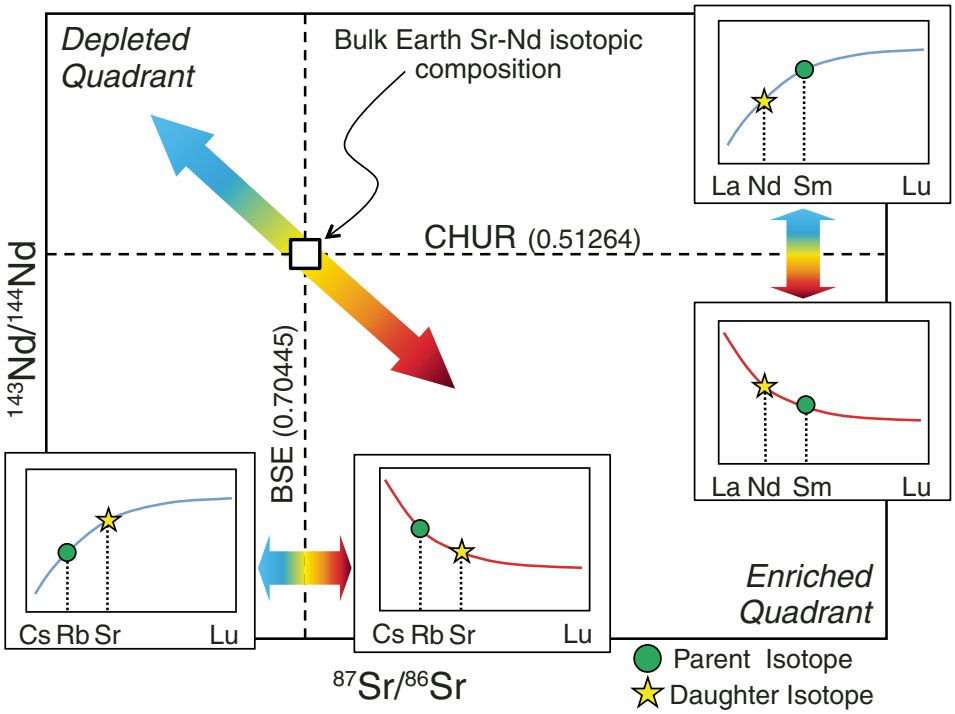

Figure 4. Schematic $^{143}Nd/^{144}Nd$ versus $^{87}Sr/^{86}Sr$ isotopic diagram reporting bulk silicate earth (BSE) and chondritic uniform reservoir (CHUR), which should represent the total average $^{87}Sr/^{86}Sr$ and $^{143}Nd/^{144}Nd$ isotopic composition of the Earth. Starting from the initial composition, partial melting produces isotopic differentiation into depleted (<BSE and >CHUR) and enriched (>BSE and <CHUR) compositions.

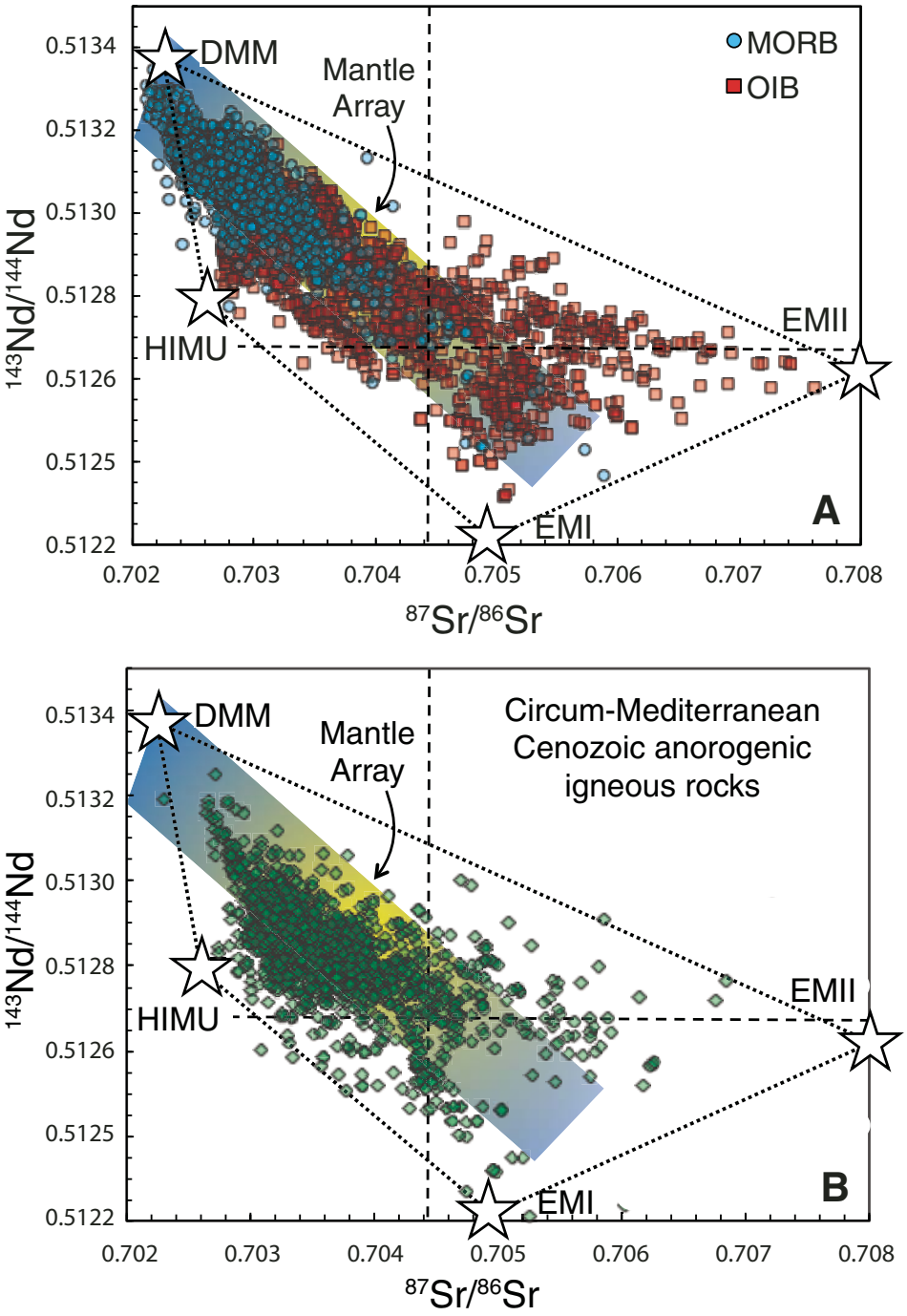

Figure 5. (A) $^{143}Nd/^{144}Nd$ versus $^{87}Sr/^{86}Sr$ isotopic diagram for oceanic basalts. (B) $^{143}Nd/^{144}Nd$ versus $^{87}Sr/^{86}Sr$ isotopic diagram for continental rocks from the circum-Mediterranean area (Lustrino and Wilson, 2007; Lustrino, 2011). In both cases all the isotopic compositions can be defined in terms of relative abundance of four main components, similar to computer printers where all the possible colors are produced using four ink cartridges (black, yellow, magenta, cyan). The background yellow strip is referred to the Sr-Nd isotopic mantle array. MORB—mid-ocean-ridge basalt; OIB—ocean-island basalt; DMM—depleted MORB mantle; HIMU—high mu, where mu = μ = $^{238}U/^{204}Pb$; EMI—enriched mantle type I; EMII—enriched mantle type II (from Stracke, 2012).

(kappa). Strictly speaking, the Greek letter μ should be spelled as "mi", not "mu". This means that the classical HIMU mantle end member should more properly be defined as "HIMI". The Earth's $^{238}U/^{235}U$ ratio is 137.88.

Given that the ^{235}U half-life is much shorter than that of ^{238}U, $^{207}Pb/^{204}Pb$ increases more rapidly than $^{206}Pb/^{204}Pb$. As a consequence, in a $^{207}Pb/^{204}Pb$ versus $^{206}Pb/^{204}Pb$ plot the Pb isotopic evolution (i.e., the Pb isotopic ratios of a rock with increasing age) follows a convex-upward curve (Fig. 6A).

Let us assume that the early Earth, with initial solar $^{206}Pb/^{204}Pb$ and $^{207}Pb/^{204}Pb$ ratios X_0 and Y_0, respectively (Fig. 6A), evolved as a single system (i.e., without any differentiation process such as partial melting) for a period t_1 with a $^{238}U/^{204}Pb$ ratio = μ_1 (Fig. 6A). After a time t_1 the new Pb isotopic composition of the Earth would be $X_{1,1}$ and $Y_{1,1}$ (Fig. 6A). If the Earth during this period had a different μ value (e.g., $\mu_2 > \mu_1$) but the same initial Pb isotopic composition, after the same time t_1 it would have had different (higher) Pb isotopic ratios ($X_{1,2}$ and $Y_{1,2}$; Fig. 6A). The dashed

line t_0-t_1, obtained by connecting the isotopic composition of different reservoirs with the same initial Pb isotopic composition, but with different μ, represents the isochron after time t_1.

What happens if the same uniform reservoirs (assumed to evolve with $^{238}U/^{204}Pb$ ratios μ_1 or μ_2 but the same initial isotopic ratios) allow Pb isotopic ingrowth for an additional time t_2? After this additional time, both the hypothetical reservoirs (with μ_1 or μ_2) will be characterized by higher $^{206}Pb/^{204}Pb$ and $^{207}Pb/^{204}Pb$ ratios. Obviously, sources with μ_2 will be characterized by more ^{206}Pb and ^{207}Pb, having higher U/Pb. At a time t_2 the Pb isotopic composition of a system with μ_1 will be $X_{2,1}$ and $Y_{2,1}$, while a system with μ_2 will be $X_{2,2}$ and $Y_{2,2}$ (Fig. 6A). The dashed line connecting t_0 and t_2 represents the isochron at t_2.

Present-day Earth (t_3 = 4.56 b.y.), with hypothetical μ_1 or μ_2, should have $^{206}Pb/^{204}Pb$ at $X_{3,1}$ and $X_{3,2}$, and $^{207}Pb/^{204}Pb$ ratios at $Y_{3,1}$ and $Y_{3,2}$, respectively (Fig. 6A). Whatever the μ of the Earth, the total Pb isotopic composition of our planet must plot on the isochron t_3. The isochron at 4.56 b.y. is defined as the meteoritic isochron or Geochron. The entire solar system (as determined by the composition of meteorites) plots on the 4.56 b.y. Geochron, with $^{206}Pb/^{204}Pb$ ratios ranging from ~10 to ~50 and $^{207}Pb/^{204}Pb$ ratios ranging from ~9 to ~37.

This, of course, does not mean that *all* the Earth's rocks must plot on the Geochron. In principle, rocks can plot on the left or on the right of the Geochron. The various shells of the Earth (crust, mantle, core) have a common origin (i.e., the same primordial solar Pb isotopic composition; X_0 and Y_0 in Fig. 6A), but have accreted or been consumed at different times and evolved with different μ values. In particular, these reservoirs evolved with different $^{207}Pb/^{204}Pb$, $^{206}Pb/^{204}Pb$, and $^{208}Pb/^{204}Pb$ ratios.

Each partial melting stage (i.e., to produce new crustal material) produces at least two different new sources characterized by different U/Pb (and μ) that will evolve quickly (high μ) or slowly (low μ), producing variable ^{207}Pb and ^{206}Pb isotopic growth. Let us assume that a uniform system evolved with primordial Pb isotopic ratios for a time t_2 and a $^{238}U/^{204}Pb$ ratio = μ_1. Its isotopic composition is indicated by the white star in Figure 6B. If a partial melting event occurs, this originally uniform system is split into two reservoirs, one evolving with low $^{238}U/^{204}Pb$ (the restitic mantle) and the other with high $^{238}U/^{204}Pb$ (the partial melt). The elemental fractionation between U and Pb happens because the two elements have slightly different compatibility in mantle minerals, and, consequentially, they are fractionated by partial melting and fractional crystallization processes.

Assuming that t_2 = 2 b.y., these two complementary reservoirs (the mantle residuum and the solidified partial melt) will evolve up to the present day with different μ, but the same initial Pb isotopic composition. After additional 2.56 b.y. (i.e., reaching present-day times), the two reservoirs will have different isotopic compositions, represented by the stars labeled R_1 (residuum) and M_1 (melt) in Figure 6B. The total Pb isotopic composition of the two systems must plot on the intersection between the Geochron and the R_1-M_1 segment (identified with X in Fig. 6B). Similarly, if the original isotopic system evolved with higher $^{238}U/^{204}Pb$ (μ_2), a partial melt extraction at t_2 = 2 b.y. will produce, at t_3 = 4.56 b.y., two systems, R_2 and M_2 (Fig. 6B). Whatever the original μ and the μ produced during partial melt formation, the total composition of the system must plot somewhere along the Geochron.

It is important to understand that the whole Earth system, not the single solid reservoirs, must plot along the Geochron. During

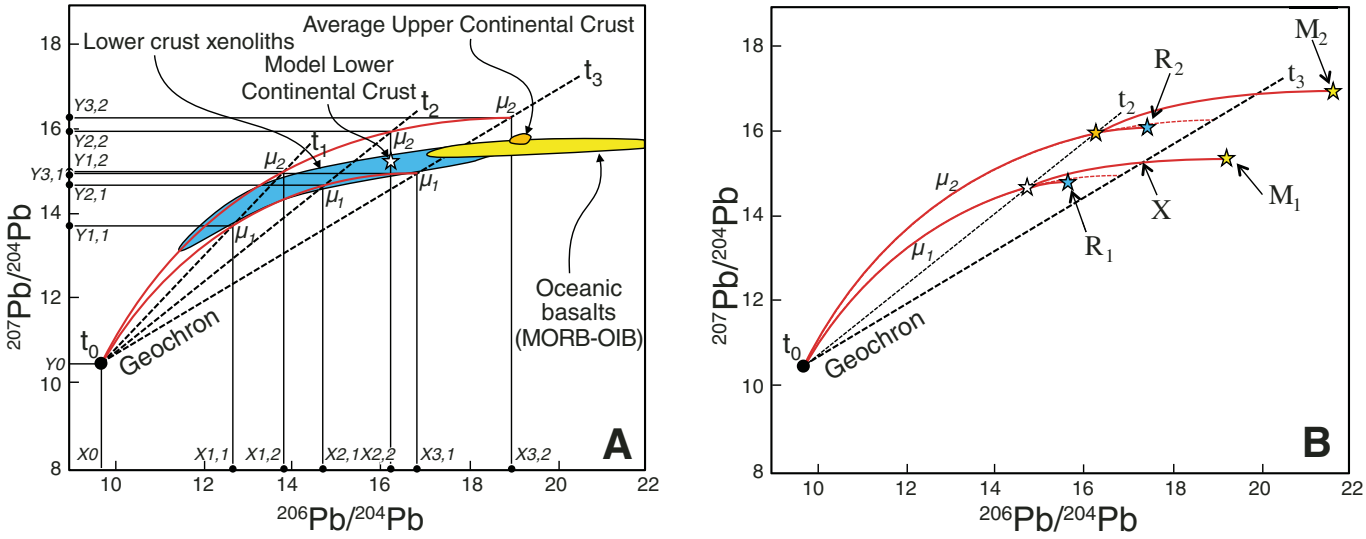

Figure 6. (A) $^{207}Pb/^{204}Pb$ versus $^{206}Pb/^{204}Pb$ isotopic diagram showing the hypothetical evolution of the Earth system starting at 4.56 Ga (t_0) with primordial (solar) $^{207}Pb/^{204}Pb$ = 10.29 and $^{206}Pb/^{204}Pb$ = 9.31, evolving with different μ values (where μ = $^{238}U/^{204}Pb$). Model lower continental crust from Bolhar et al. (2007). Lower and upper continental crust fields from references reported in Lustrino (2005) and Bolhar et al. (2007). References for oceanic basalt field are from Stracke (2012). MORB—mid-ocean-ridge basalt; OIB—ocean-island basalt. (B) $^{207}Pb/^{204}Pb$ versus $^{206}Pb/^{204}Pb$ isotopic diagram illustrating the effect of partial melt extraction (producing melts M_1 and M_2 and solid residua R_1 and R_2).

the Earth's chemical stratification, the upper crust evolved with higher U/Pb (given that U is slightly more incompatible than Pb during partial melting processes) and the residual mantle evolved toward lower U/Pb. This, coupled with the different initial Pb isotopic compositions of these two most extreme reservoirs, means that ancient upper crustal rocks, having higher U/Pb, are also characterized by higher μ and, consequentially, should plot somewhere to the right of the Geochron.

On the other hand, residual mantle rocks, characterized by lower μ, should have retarded ^{207}Pb and ^{206}Pb isotopic growth, and consequentially they should plot to the left of the Geochron. What is anomalous is that both upper crustal rocks (various estimates grouped in the small orange field in Fig. 6A) and depleted mantle rocks (or partial melts, i.e., MORB; part of the yellow field in Fig. 6A) all plot to the right of the Geochron. Also >99.9% of OIB plot on or to the right of the Geochron (OIB and MORB are grouped in the same yellow field in Fig. 6A). This is called the first Pb paradox (Allegre, 1968).

If both partial melts and residual mantle compositions all plot to the right of the Geochron, some hidden or poorly represented reservoir must exist somewhere. This reservoir must be placed well to the left of the Geochron, so that the whole Earth Pb isotopic composition plots somewhere along this line. The only terrestrial reservoir characterized by compositions plotting to the left of the Geochron (and characterized by low to extremely low ^{206}Pb/^{204}Pb, down to ~10, and μ ~0) is the ancient lower continental crust.

In Figure 6A both the fields of ancient lower crustal xenoliths (sky blue field) and the model old continental crust (star; Lustrino, 2005; Bolhar et al., 2007) are shown. The metamorphic reactions occurring during basalt to granulite-eclogite facies are indeed characterized by U/Pb fractionation, with U leaving the system more easily than Pb. The consequence is that a metamorphosed (eclogitic, or any plagioclase-free high pressure metamorphic equivalent of basaltic rocks) lower crust is characterized by very low μ, and consequentially its ^{206}Pb/^{204}Pb (but also ^{207}Pb/^{204}Pb) remains virtually frozen and does not increase with time, as there is little if any ^{238}U (and ^{235}U). If such an eclogitization process is old, the Pb isotopic ratios are stopped at their infant stage, close to values more similar to primordial solar system values (^{206}Pb/^{204}Pb = 10.29; ^{207}Pb/^{204}Pb = 9.31) than the typical igneous rock range (^{206}Pb/^{204}Pb = ~17–21; ^{207}Pb/^{204}Pb = ~15.2–15.8; μ = 4–16).

Foundering of this dense lithology (which is denser than the shallow lithospheric mantle) in the form of a mafic keel in overthickened collision zones can explain the extreme rarity of these compositions on the Earth's surface. This dense eclogite may be now stored in the transition zone, as originally proposed by Anderson (1989).

The lead isotope system is particularly important in basalt petrogenesis especially because it is considered to be one of the milestones of geochemical mantle plume modeling, suggesting lower mantle derivation for OIB. Ironically, it was Pb isotopes that led Tatsumoto (1978) to conclude that OIB was from the shallow mantle and MORB from the deeper mantle, thus agreeing with the classical physics-based models (e.g., Birch, 1952).

Two of the four "colors" of the Earth's mantle (i.e., the mantle end members manifested in oceanic basalts away from subduction zones) are essentially identified on Pb isotopic grounds. One of these colors is represented by the EMI end member (e.g., Lustrino and Dallai, 2003), whose type localities are identified in the Pitcairn Islands and seamounts in French Polynesia (e.g., Woodhead and Devey, 1993), the east-central Atlantic Ocean (Walvis Ridge; Salters and Sachi-Kocher, 2010), some southwest Indian Ocean ridge sectors, the Afanasy-Nikitin seamount chain (SW India) (Mahoney et al., 1996; Borisova et al., 2001), and the Ko'olau-stage lavas of Oahu island (Hawaii; Tanaka et al., 2002; Huang and Frey, 2005). This hypothetical mantle end member is characterized by its peculiar low ^{206}Pb/^{204}Pb (down to ~16.7; Fig. 7), associated with non-unique mildly radiogenic ^{87}Sr/^{86}Sr and strongly unradiogenic ^{143}Nd/^{144}Nd (Fig. 5).

The other mantle color (end member) defined on the grounds of Pb isotopes is HIMU, represented by a very rare group of rocks cropping out in French Polynesia (Rurutu, Tubuai, and Mangaia islands; Chauvel et al., 1995; Stracke et al., 2005; Hanyu et al., 2013) and, with less extreme compositions, on the island of Saint Helena (southern Atlantic Ocean); Kawabata et al., 2011; Hanyu et al., 2014). The HIMU end member is characterized by the most radiogenic Pb isotopic compositions recorded in oceanic basalts (Fig. 7A). The other two colors of the mantle isotopic printer are EMII and DMM.

The EMII mantle end member is characterized by ^{206}Pb/^{204}Pb intermediate between EMI and HIMU (~19) and relatively high ^{207}Pb/^{204}Pb for a given ^{206}Pb/^{204}Pb (Fig. 7A). The relative ^{207}Pb/^{204}Pb enrichment of EMII lavas can be mathematically shown as a positive Δ7/4Pb value, a parameter proposed by Hart (1984) to emphasize the vertical shift of Southern Hemisphere oceanic basalts compared with northern ones (defining the so-called NHRL, Northern Hemisphere Reference Line) in ^{207}Pb/^{204}Pb versus ^{206}Pb/^{204}Pb plots (Fig. 7A). The vertical shift from the NHRL (that can be identified also for ^{208}Pb/^{204}Pb; Δ8/4Pb) is also defined as the DUPAL anomaly (after the two researchers who first described it; Dupré and Allègre, 1983).

The last color of the mantle isotopic printer is DMM (Fig. 7A). This color is by far the most common and nearly always present in portraits of oceanic and continental intra-plate basalts. It is also a constant feature of partial melts generated in suprasubduction mantle wedges. Despite the fact that DMM is necessary in almost every recipe to model oceanic basalts, the Pb isotopic composition of DMM is not well constrained. Indeed, there have been several attempts to estimate the ^{206}Pb/^{204}Pb, ^{207}Pb/^{204}Pb, and ^{208}Pb/^{204}Pb of this end member, with estimates ranging from ~16.8 to ~18.4 (^{206}Pb/^{204}Pb), from ~15.3 to ~15.4 (^{207}Pb/^{204}Pb), and from ~36.5 to ~38 (^{208}Pb/^{204}Pb). The quadrilateral with the four mantle end members at the apexes also envelops continental rocks, as shown in Figure 7B. Surprisingly, from a mantle plume point of view, DMM is not a focal point on isotope plots, i.e., trends do not converge toward DMM compositions. They

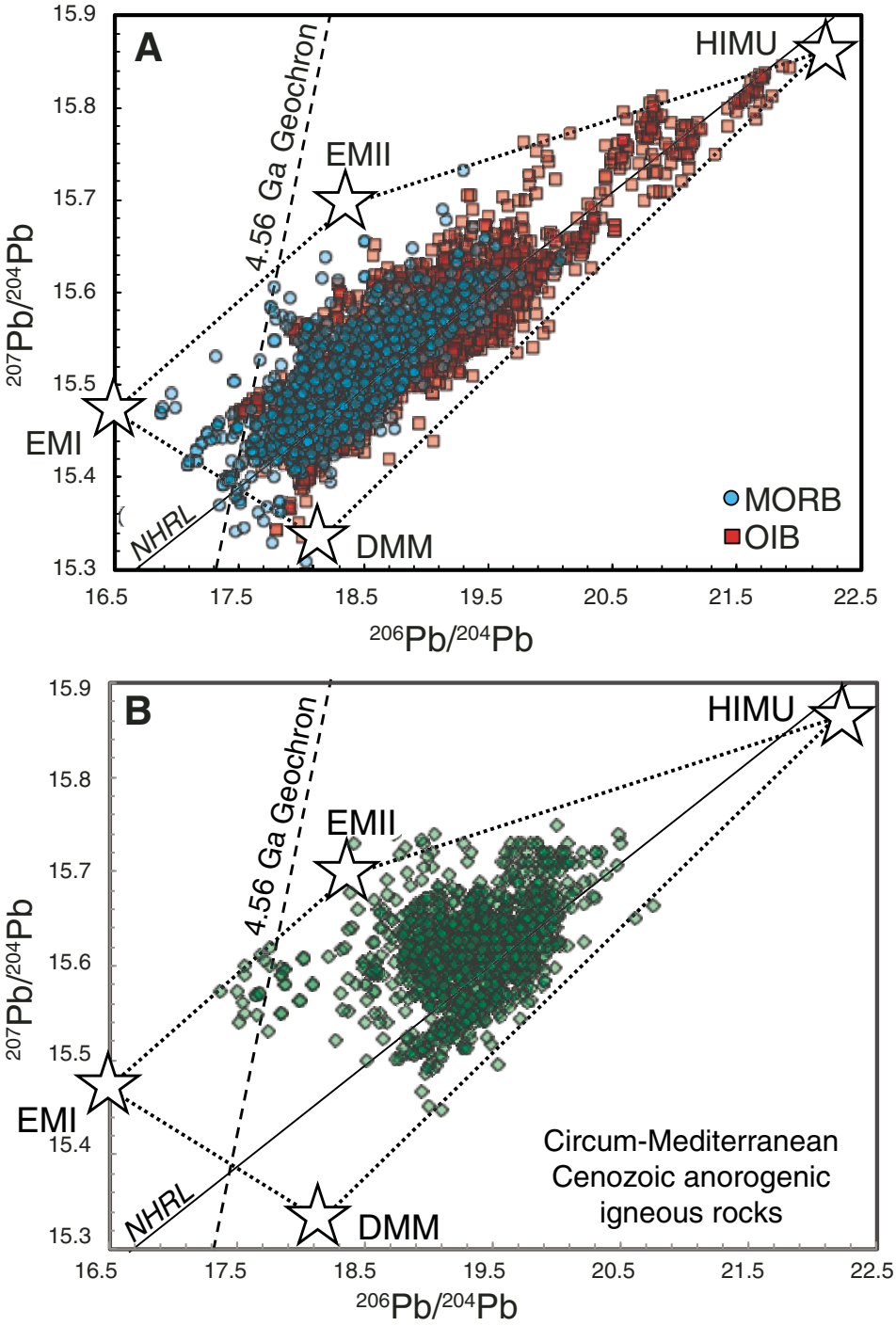

Figure 7. (A) $^{207}Pb/^{204}Pb$ versus $^{206}Pb/^{204}Pb$ isotopic diagram for oceanic basalts (references in Stracke, 2012). Worth noting is the nearly complete overlap of mid-ocean-ridge basalt (MORB) with ocean-island basalt (OIB) and the position to the right of the Geochron of nearly all the compositions. Also in this case, the Pb isotopic ratios of oceanic basalts can be defined in terms of only four end members (the isotopic colors of the mantle printer): DMM—depleted MORB mantle; HIMU—high mu, where mu = $\mu = {}^{238}U/^{204}Pb$; EMI—enriched mantle type I; EMII—enriched mantle type II. NHRL is the Northern Hemisphere Reference Line (Hart, 1984), which represents the average Pb isotopic composition of the Northern Hemisphere oceanic basalts. The vertical shift (negative or positive) from this line is defined by the parameter Δ7/4Pb. (B) $^{207}Pb/^{204}Pb$ versus $^{206}Pb/^{204}Pb$ isotopic diagram for continental intra-plate volcanic rocks from the circum-Mediterranean area; references in Lustrino and Wilson (2007) and Lustrino (2011). The complete list of the analyses (>8000 rocks) reported in Fig. 7B is available on request to the first author.

converge toward FOZO (focal zone) or C (common component; Stracke et al., 2005; Jackson et al., 2014).

The Sr-Nd isotopic resemblance between DMM and HIMU (plotting in the same depleted field) disappears when observing these two end members from different perspectives (i.e., Pb isotopes). Figure 7 clearly indicates their different origins. The position of the DMM reservoir is compatible with a U-depleted composition, while the extremely radiogenic $^{206}Pb/^{204}Pb$ (but also of the other Pb isotopic pairs) of the HIMU end member requires high U/Pb and Th/Pb in its genesis. This is classically attributed to recycling of Pb-poor lithologies in the deep mantle, in regions not involved in strong convective systems (e.g., Chauvel et al., 1992, 1995). These Pb-poor lithologies probably are hydrothermally altered oceanic crust where Pb was first concentrated in sulfides which were then removed when the slab entered the trench. The oceanic crust residuum would be, as a consequence,

characterized by high U/Pb, not because of elevated U content, but rather because of low Pb. Storage of such high U/Pb lithologies and insulation for long periods would allow radiogenic growth of ^{206}Pb and ^{207}Pb, which are the most striking characteristics of the HIMU end member (Fig. 7). In other words, the Pb isotopic composition of the HIMU end member (classically identified as the strongest geochemical evidence for a mantle plume) requires long periods of insulation of high U/Pb lithologies, not thermal anomalies or deep sources. With the present state of knowledge, it is not possible to say that a given Pb isotopic composition is proof for the existence of a mantle plume as often used as an *a priori* conjecture.

The U-Th-He Isotope System

Helium is the lightest noble gas, present in two isotopes, ^{3}He and ^{4}He, whose ratios in igneous rocks are classically used to constrain mantle structure and infer its evolution (e.g., Ballentine, 2012). ^{3}He is the primordial isotope trapped inside the Earth during its accretion, and is continuously escaping from the Earth's surface when mantle melts degas at shallow depths. During the decay into stable Pb isotopes, ^{235}U, ^{238}U, and ^{232}Th produce ^{4}He isotopes as α-particles. Helium isotopes are classically reported as ^{3}He/^{4}He ratios (R) over atmospheric ^{3}He/^{4}He ($R_A = 1.38 \times 10^{-6}$ cm^3/g). This reverses the usual geochemical convention of the radiogenic isotope (e.g., ^{87}Sr or ^{143}Nd) normalized to the stable isotope (e.g., ^{86}Sr or ^{144}Nd). In the case of helium the stable isotope (^{3}He) is normalized to the radiogenic one (^{4}He). This convention is carried over into the interpretation of ^{3}He/^{4}He ratios where variation in ^{4}He is usually not considered and high ^{3}He/^{4}He is typically attributed to high ^{3}He derived from a deep-sourced, undegassed mantle region (e.g., Davies, 2011). Despite increasing criticism in using He isotope systematic to infer the existence of primordial deep mantle reservoirs for "plume magmas" (White, 2010), high ^{3}He/^{4}He ratios in basaltic melts continue to be considered the strongest isotopic signal of a deep mantle provenance of their sources (Jackson et al., 2014).

MORB are characterized by ^{3}He/^{4}He ratios (R/R_A) ranging from ~1 to ~22, but with nearly all the samples concentrated in the narrow interval 8 ± 1 R/R_A (e.g., Meibom et al., 2003; Graham et al., 2014). In contrast to MORB, magmas emplaced in oceanic and continental intra-plate settings are characterized by variable ^{3}He/^{4}He ratios, with R/R_A ranging from ~5 to ~50 and a poor correlation with other isotope systematics and incompatible trace element ratios (e.g., Peters and Day, 2014). This can be understood in part from the central limit theorem (high-degree melts and large-volume samples average over large volumes and have smaller variances) and from the fact that helium isotope ratios are partly controlled by degassing as well as by melting (Meibom et al., 2003).

Earth materials are characterized by ^{3}He/^{4}He ratios much lower (<50 R/R_A) than the cosmic solar wind (~310 R/R_A) because of the continued ^{3}He loss and the continued ^{4}He production by radioactive decay. Plate tectonics moves primordial ^{3}He from the Earth's interior to the surface via partial melting and degassing, while subduction recycles back to the mantle ^{4}He in the form of (U + Th)–rich crustal lithologies. The result is that the ^{3}He/^{4}He ratio of the Earth has been continuously decreasing since the Earth's accretion (Fig. 8A). The two exceptions are in sediments that are rich in cosmic spherules (solar ^{3}He rich) and in lithium-rich rocks (e.g., Smith, this volume).

Despite the common view (e.g., Gonnermann and Mukhopadhyay, 2009; Davies, 2011; Ballentine, 2012), high ^{3}He/^{4}He ratios indicate high time-integrated ^{3}He/(U + Th) ratios, not automatically high absolute ^{3}He content. Similarly, low ^{3}He/^{4}He ratios are not proof of absolute low ^{3}He content. Relatively low ^{3}He/^{4}He ratios in MORB have been related to relatively (U + Th)–rich concentrations associated with variable He loss through magma degassing in the upper mantle (i.e., ^{4}He rich rather than ^{3}He poor; Meibom et al., 2003) and the presence of He-rich bubbles trapped in cavities and nucleating on the surface of early-forming olivine crystals (Natland, 2003). Similarly, high ^{3}He/^{4}He ratios can result from ancient (U + Th)–poor sources, resulting in low ^{4}He production with time, while low ^{3}He/^{4}He ratios can result from sources with ancient (U + Th)–rich lithologies.

Despite these obvious considerations, the scientific literature is full of claims such as: "Helium is a powerful tracer of primitive material in Earth's mantle. Extremely high ^{3}He/^{4}He ratios in some ocean-island basalts suggest the presence of relatively undegassed and undifferentiated material preserved in Earth's mantle" (Jackson et al., 2010, p. 853); "Hot-spot magmas often have elevated values in the ratio of primordial helium to radiogenic helium (^{3}He/^{4}He), which indicates their source is in a part of the Earth that has not lost its dissolved gases to the atmosphere" (Humphreys and Schmandt, 2011, p. 34); "The existence of different ^{4}He/^{3}He ratios underpins the idea that there are at least two geochemical reservoirs in the mantle: a deep reservoir rich in gases and volatile compounds feeds material into an upper reservoir, which is the convecting part of the mantle that supplies magma to mid-ocean ridges" (Ballentine, 2012, p. 40); "[...] the less-degassed mantle source traced by high ^{3}He/^{4}He. [...] He isotopes provide direct evidence for the preservation of relatively undegassed, primordial reservoirs in the present-day mantle" (Peters and Day, 2014, p. 4).

More evolved views interpret both high ^{3}He/^{4}He and low ^{3}He/^{4}He ratios as being derived from deep mantle plumes, the first representing the true plume matrix and the second representing the "subducted materials—oceanic crust, mantle lithosphere and sediments—which may also reside in slab graveyards at the bottom of the mantle where plumes originate" (Jackson et al., 2014, p. 357). In other words, whatever ^{3}He/^{4}He ratios are measured in mantle melts (as low as 5 or as high as 50 R/R_A), they are considered to represent proof for a deep mantle provenance.

Focusing on the elemental He content in basalt phenocrysts (mostly clinopyroxene and olivine), it emerges that OIB have a much lower ^{3}He (typically around 10^{-14} to 10^{-11} cm^3/g) compared with MORB (typically around 10^{-11} to 10^{-9} cm^3/g; Ozima and Igarashi, 2000; Hanyu et al., 2005; Mourao et al., 2012; Hanyu,

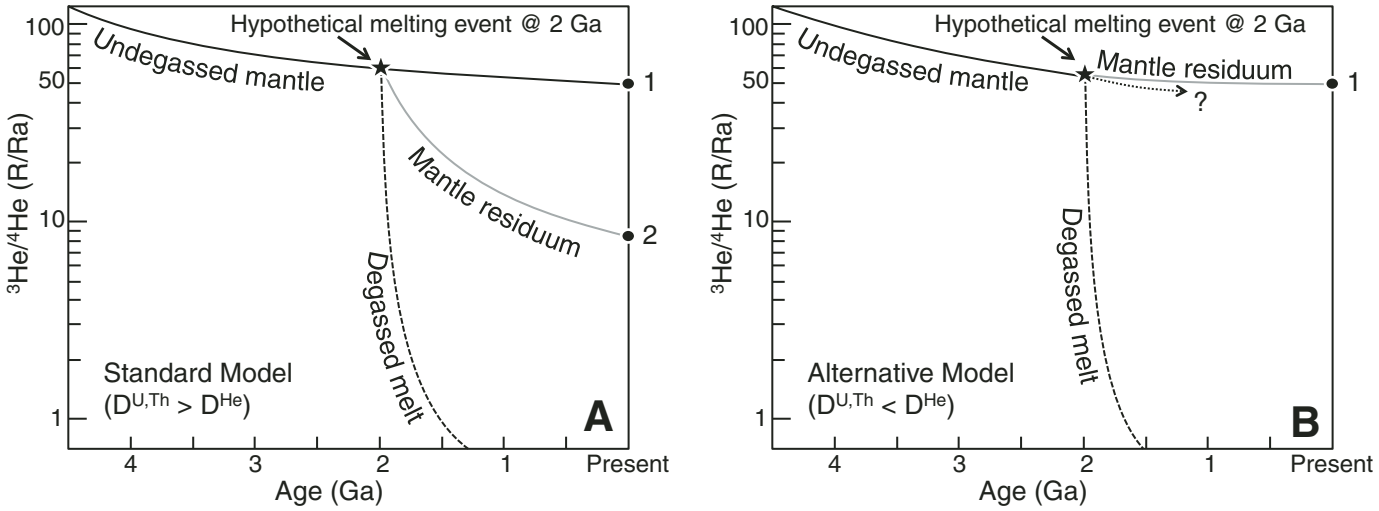

Figure 8. (A) Classical interpretation of isotopic evolution of the $^{3}He/^{4}He$ system with age. The $^{3}He/^{4}He$ ratio decreases continuously because of progressive ^{3}He escape and ^{4}He production by Th-U decay into stable Pb isotopes. An undegassed Earth (i.e., primitive mantle composition) would today be characterized by $^{3}He/^{4}He$ around 50 R/R_A (black dot 1), where R is the isotopic ratio measured in the rock and R_A is the same ratio measured in the present-day atmosphere. D is the bulk distribution coefficient in the melting assemblage and quantitatively indicates the tendency of an element to remain into the solid (high D, high compatibility) or to preferentially partition into the melt (low D, high incompatibility). According to this view, He is more incompatible than U + Th during partial melting, resulting in a $^{3}He/(U + Th)$–poor mantle residuum (black dot 2). The melt will experience substantial degassing, resulting in strong ^{3}He depletion (dashed line). (B) Alternative model of $^{3}He/^{4}He$ isotopic evolution, assuming stronger incompatibility of U + Th compared with He. In this case the solid residuum would be characterized by higher $^{3}He/(U + Th)$, leading to higher $^{3}He/^{4}He$ compared with undegassed melt. Modified from Parman et al. (2005).

2014). Despite this, it is commonly believed that "The MORB source contains less ^{3}He because it was degassed in early Earth history" (Moreira et al., 2012, p. 91) and that high $^{3}He/^{4}He$ ratios reflect lower mantle chemical signatures in continental settings (e.g., the Columbia River Basalt Group; Camp, 2013). There is no reason to believe that MORB sources are depleted in ^{3}He compared with postulated primitive and undegassed plume–related OIB sources (Anderson, 1998, 2007; Ozima and Igarashi, 2000). On this basis, statements such as "Large, long-lived, ^{3}He-rich plumes, and especially those that have generated enormous volumes of oceanic or continental flood basalts, are more likely to have come from the base of the lower mantle" (Hofmann, 1997, p. 228) need rethinking. The actual very low ^{3}He content of postulated "plume magmas" (i.e., up to five orders of magnitude less than what is recorded in MORB) has been related to the subaerial activity of OIB, a characteristic that would favor preferential noble gas escape from magma compared with MORB, erupted at high water depths (and therefore high pressures, preventing degassing). This solution is not viable because OIB should also have much higher $^{3}He/^{36}Ar$ than MORB (the higher the mass of the noble gas, the less its melt compatibility; e.g., Carrol and Draper, 1994), while actually MORB are characterized by higher $^{3}He/^{36}Ar$ ratios, with no correlation between ^{3}He and ^{36}Ar (Ozima and Igarashi, 2000). The fact that the highest $^{3}He/^{4}He$ ratios (~50 R/R_A) are recorded in Mg-rich, alkali-poor picritic magmas (Baffin Island, northeastern Canada, characterized by very low $^{87}Sr/^{86}Sr$ [~0.7031] and very high $^{143}Nd/^{144}Nd$ [~0.5130]; Stuart et al., 2003) indicates an important role of depleted mantle sources in their petrogenesis. The depleted (i.e., not primitive nor undegassed) source is also testified by low LREE/MREE ratios (LREE, light REE; MREE, medium REE; e.g., La/Sm <0.6).

The apparent conundrum of invoking undegassed sources in the petrogenesis of alkali-poor, Sr-unradiogenic and Nd-radiogenic basaltic melts is solved by proposing mixing between depleted upper mantle (responsible for all the geochemical characteristics of the Baffin Island picrites, also apparent in the mineral chemistry) and a gas-rich (^{3}He-rich) component (Stuart et al., 2003). The linear correlation between He-Sr and He-Nd isotopes should indicate a perfect He elemental distribution in the two mixing end members, which is difficult to understand invoking DMM and primitive mantle regions (as a plume head dispersed in the upper mantle) to represent these two end members. The Baffin Island picrites are important because they are considered to be the first product of the proto-Icelandic mantle plume (e.g., Graham et al., 1998; Stuart et al., 2003; Jackson et al., 2010).

The mantle plume hypothesis has received support from the conclusions of many noble gas geochemists who have proposed a direct link between high $^{3}He/^{4}He$ ratios with high absolute ^{3}He and, as a consequence, a primitive and relatively undegassed source (Class and Goldstein, 2005; White, 2010; Jackson et al., 2010; Ballentine, 2012). Alternatively, the origin of a ^{3}He-rich lower mantle is considered not a primary feature, but, rather, related to accumulation of recycled oceanic basalts and hybrid pyroxenites rich in ^{3}He (Davies, 2011). The supposed high abundance in ^{3}He of oceanic crust recycled down to D″ is based on the assumption that He is strongly partitioned to melts during

shallow mantle melting beneath oceanic ridges. While this is certainly true, this model cannot explain (1) the differences between MORB and "lower mantle–derived" OIB; (2) the lower absolute abundance of ^{3}He in OIB compared to MORB, and (3) the radiogenic ingrowth of ^{4}He due to the decay of U and Th isotopes that would decrease the ^{3}He/^{4}He in the mantle plume–related OIB.

In some cases ^{3}He/^{4}He ratios in the range 6.5–10.6 R/R_A and ^{3}He contents as low as 10^{-14} cm^3/g have been considered, together with other noble gas arguments, as sufficient proof for the presence of deep-rooted mantle plumes below Hawaii and the Louisville seamount chain in the southwest Pacific Ocean (Hanyu, 2014). According to this view, the U-Th-He isotopic system is related to the different compatibility of U + Th with respect to He in rocks and magmas (degassing fractionation between U, Th, He, and other noble gases being ignored). The two different approaches are reviewed by Parman et al. (2005; Figs. 8A, 8B). The continuous thick line evolving from ~130 R/R_A (at ~4.5 Ga) to ~50 R/Ra (at present) indicates the evolution of a (U + Th)–bearing undegassed mantle. Partial melts of this undegassed mantle should be characterized by relatively high R/R_A values, indicated with black dot 1 in Figures 8A and 8B (representing the highest ^{3}He/^{4}He measured in igneous rocks; Stuart et al., 2003). A hypothetical partial melting event at 2 Ga would produce a liquid and a mantle residuum. Both He and the U + Th pair are strongly incompatible during mantle partial melting, but the standard model assumes stronger incompatibility of He with respect to both U and Th. This means that partial melts have higher He/(U + Th) than either the undegassed mantle or the mantle residuum. Such a partial melt would be subject to degassing at shallow depths, allowing preferential escape of He from the melt and resulting in a ~1000-fold reduction of the original He/(U + Th) ratio (Parman et al., 2005). The isotopic evolution of this degassed melt is indicated with the dashed line in Figure 8A. The mantle residuum would be characterized by lower He/(U + Th) ratios than undegassed mantle and partial melts. The evolution of this depleted (degassed) reservoir would evolve toward relatively low ^{3}He/^{4}He (R/R_A ~8) like that recorded in present-day MORB (Fig. 8A). In the alternative model, U and Th are up to two orders of magnitude more incompatible than He during partial melting ($D^{Th,U} < D^{He}$; where D is the bulk partition coefficient; Parman et al., 2005). The partial melt would evolve more or less in the same way as in the standard model, with shallow-depth magma degassing the controlling mechanism to produce He-poor, He/(U + Th)–poor melts evolving with age toward very low ^{3}He/^{4}He ratios. The difference from the standard model rests in the fact that in this case the degassed reservoir (mantle residuum) would be characterized by higher ^{3}He/^{4}He than both partial melt and undegassed mantle, because it is characterized by higher He/(U + Th) ratios (black dot 1 in Fig. 8B). The petrological implications for this alternative model are particularly relevant. ^{3}He/^{4}He values as high as 50 R/R_A would reflect not primitive (undegassed) mantle sources but derivation from depleted residua (Parman et al., 2005). Partial melting effectively cannot decrease He/(U + Th) ratios in the mantle residuum, and high He/(U + Th) ratios can develop in mantle residua through large extents of melting, but at the same time are associated with low He (and other noble gases) concentrations (Jackson et al., 2013).

In conclusion, both high and low ^{3}He/^{4}He ratios can be associated with recycling processes. Low ^{3}He/^{4}He requires the presence of an old (U + Th)–rich component (e.g., recycled crust or sediment), while high ^{3}He/^{4}He ratios can be explained by recycling of refractory peridotite or olivine-rich cumulates (rich in gas-filled bubbles or cracks; e.g., Natland, 2003; Anderson, 2007). In either case, recycling down to the lower mantle is not required.

INK CARTRIDGES IN THE MANTLE ISOTOPIC PRINTER

^{87}Sr/^{86}Sr ratios of HIMU and HIMU-like OIB are all lower than that of BSE. This characteristic is at odds with derivation from a primitive (i.e., never tapped by basaltic extraction) source. This conundrum has been explained by derivation from a deep mantle source that interacted with low-^{87}Sr/^{86}Sr recycled oceanic crust (e.g., Hofmann, 1997, 2003). The low-^{87}Sr/^{86}Sr characteristic is intrinsic of a partial melt generated from a depleted (DMM) source in which Rb, more incompatible than Sr during melt extraction, is preferentially transferred to the melt. If such a depleted, low-Rb/Sr source partially melts again, the new liquid is characterized by low ^{87}Rb/^{86}Sr, and consequentially evolves toward low ^{87}Sr/^{86}Sr isotopic ratios. Low Rb has also been postulated as a consequence of hydrothermal alteration of oceanic crust that concentrates this metal in secondary veins that are easily mobilized during the first stages of dehydration metamorphic reaction occurring at shallow depths below the supra-subduction lithospheric mantle wedge (e.g., Chauvel et al., 1992).

Ancient recycling (of the order of 2 b.y. and more) of MORB-like lithologies (characterized by low to very low Rb/Sr and thus low to very low ^{87}Sr/^{86}Sr) would have reduced the ^{87}Sr/^{86}Sr of the primitive deep mantle from BSE values to values indistinguishable from present-day MORB.

The EMI-EMII OIB ^{87}Sr/^{86}Sr ratios higher than that of BSE have been explained by derivation from a deep mantle that interacted with high-^{87}Sr/^{86}Sr lithologies in the form of subducted sediments (pelitic and terrigenous) and delaminated and/or eroded lower continental crust (e.g., Zindler and Hart, 1986; Lustrino and Dallai, 2003; Stracke et al., 2005; Jackson and Dasgupta, 2008; Willbold and Stracke, 2010; Stracke, 2012). What is interesting is that in some cases (e.g., HIMU-like basalts), the contribution of "normal" oceanic crust is dominant (low ^{87}Sr/^{86}Sr) compared to the geochemical (and isotopic) budget of altered oceanic crust (characterized by much higher Rb/Sr ratios) or the thin sediment veneer (e.g., White, 2010; Stracke, 2012). In all three cases, the HIMU, EMI, and EMII components (actually isotopic "flavors") provide evidence of variable interaction with a shallow DMM-like mantle, producing the various "colors" recorded in intra-plate oceanic basalts.

In summary, the isotopic compositions of three of the main four "ink cartridges" of the mantle isotopic printer (HIMU,

EMI, and EMII) are essentially related to recycling of subducted lithologies (fresh versus altered oceanic crust, pelitic versus terrigenous sediments, plus variable contribution of metasomatically modified oceanic lithospheric mantle) or tectonic erosion of the base of the supra-subduction continental mantle wedge (e.g., Clift and Vannucchi, 2004; Willbold and Stracke, 2010). Alternative but similar views interpret these three "colors" as partial melts or ancient gases frozen in the shallow boundary layer (e.g., Natland, 2003; Anderson, 2007; Niu et al., 2011; Pilet et al., 2011; Pilet, this volume). These interpretations, albeit with several necessary distinctions and case-by-case peculiarities, are valid. The models explaining the significance of the geochemical mantle zoo (Stracke et al., 2005) can be grouped into two categories. One considers that the most peculiar isotopic characteristics of the mantle end members reflect recycling (both directly, in the form of subducted lithologies, or indirectly, in the form of tectonically eroded lithospheric sole) of material once stored at shallow depths or at the Earth's surface (e.g., Hofmann, 2003; White, 2010; Stracke, 2012). The second considers that Na-K-H-C–rich partial melts infiltrating the shallow mantle can metasomatize the lithospheric mantle and are not necessarily related to subduction tectonics (e.g., Niu and O'Hara, 2008; Pilet, this volume). Whichever is correct, the isotope systematics do not require deep mantle sources nor temperature excesses. This means that any mantle plume hypothesis based on geochemical arguments is fundamentally suspect.

According to the standard geochemical model, the isotopic cartridges of the mantle printer are in the deepest mantle because this is the only place not involved in vigorous convection (Fig. 1B). The peculiar isotopic characteristics of the various mantle end members are explained by isolation from convection. This need for isolation actually applies more to the MORB source than to hypothetical plume sources. What would be the difference if the recycled lithologies are stored not in the deeper mantle, but in the upper thermal boundary layer (B″ in Fig. 1B, also known as perisphere or LLAMA)? There would be no difference at all.

Having four ink cartridges close to the Earth's surface in the shallowest mantle and the transition zone also has the advantage that there is then no need to assume the thermal state, chemical composition, and rheological behavior of the deep mantle, for which there is little supporting evidence. Because of the low temperatures and high strength at the top of the upper boundary layer, ionic diffusivities are very low and even ancient He isotope signatures can be preserved.

What is necessary in the geochemical mantle plume model is the presence of regions in the Earth's interior that escape continuous homogenization. In order to allow a given isotopic ratio to grow, the source (isotopic color) must be placed somewhere (ink cartridge) and reside there until it is tapped. Three of the four ink cartridges (as identified by different isotopic systematics) can certainly be placed in the upper 150–250 km of the mantle.

Concerning the volume of magma production associated with postulated mantle plumes, it is sufficient to consider the following. Assuming the presence of only 2% melt in a 100-km-thick seismic low-velocity zone (e.g., the LLAMA volume of Anderson [2011]), the estimated amount of melt there is of the order of 10^9 km^3. This amount is ample to explain the volumes erupted in typical OIB or large igneous province eruptions (e.g., Mahoney and Coffin, 1997; Cañón-Tapia, 2010).

CONCLUDING REMARKS

Various petrogenetic models have been proposed to explain the presence, the abundance, the physical state, and the origin of the four principal mantle end members (DMM, HIMU, EMI, and EMII) in the oceanic mantle. These end members, based on Sr-Nd-Pb isotope systematics, represent the most extreme compositions that can be found in the oceanic mantle. Extreme values occasionally found in magmas emplaced in continental settings can be related to interaction of mantle partial melts with isotopically extreme crustal lithologies.

We interpret these end members using the analogy of printing, where four basic colors (black, cyan, magenta, yellow), mixed in the appropriate amounts, can produce the full range of colors. Similarly, assuming four isotopic mantle end members, it is possible to produce the whole range of oceanic basalt isotopic compositions. All of the "colors" are present in a relatively restricted area east of Australia, in the Polynesia-Melanesia-Micronesia region. In some cases they are present virtually in the same volcanic district (e.g., Jackson et al., 2014), rendering the possibility of a provenance from the D″ region (without complete mixing of the "colors") at least dubious. With the exception of DMM, all the other mantle end members require the involvement of olivine-poor lithologies. These lithologies have been identified in upper and lower crustal rocks, recycled oceanic crust, terrigenous and/or pelagic sediments, kimberlites, carbonatites, sulfides, oxides, or frozen basaltic melts crystallized at depth (e.g., Ivanov, this volume; Pilet, this volume; Smith, this volume).

Geochemists and petrologists now generally agree on the origin of these colors. The great differences in opinion lie in where the "isotopic cartridges" are considered to be located in the Earth's interior. Thermal anomalies are not associated with these end members, nor are they required in any form. A small degree of melting is sometimes invoked to explain absolute trace element contents or the trace element fractionation recorded in lavas. Shallow degassing and contamination is implied in noble gas systematics. Helium isotopes cannot be used to constrain the existence of an undegassed lower mantle or the physical conditions of deep mantle upwellings. Extensive overlap of MORB and OIB in terms of Sr-Nd isotopic ratios and nearly complete overlap in Pb isotopes indicate that the mantle sources are not necessarily very different in terms of depth or insulated from each other.

Shallow anomalies are responsible for intra-plate volcanism. Mantle plumes and a fully convecting mantle are unproven assumptions. Physically realistic Earth models have a thick upper thermal boundary layer, characterized by superadiabatic thermal gradient, with a thickness of the order of 100–200 km. Three out of the four mantle "colors" (HIMU, EMI, and EMII) can be drawn

from this region of the Earth, which is also mobilized by shallow convection associated with plate tectonics. The fourth color, by far the most abundant, is represented by DMM and probably comprises the shallow mantle matrix or, as recently proposed, passive mantle updraft from the transition zone (Anderson and Natland, 2014). This thermodynamically self-consistent model eliminates the need for lower mantle involvement in oceanic basalt petrogenesis and surface igneous activity in general. All of the isotopic color cartridges can be placed at shallow depths, and tapping of lower mantle is not required.

ACKNOWLEDGMENTS

Don passed away during the corrections of the last draft of this manuscript. It is an immense honor for me (ML) to have had the opportunity to coauthor a paper with such a giant of the Earth Sciences. This manuscript is dedicated to Democritus (fifth century B.C.), considered the father of the modern science. This ancient Greek philosopher understood the atomistic nature of matter and spent his life fighting dogma. For this reason, more than 99% of his products have been lost, destroyed by religious communities. The Democritus philosophical approach luckily survived, at least partially, in the ancient Greek philosopher Epicurus (third century B.C.), and, above all, the great Latin poem "*De Rerum Natura*" of Lucretius (first century B.C.). I find that love for the truth, obstinate hate against dogma, and genius constitute solid connecting lines between Democritus and Don Anderson.

ML thanks MIUR PRIN (MP) (2010 20107ESMX9_001) and Ateneo La Sapienza (Fondi Ateneo, 2013, 2014) for financial support. ML greatly enjoyed discussions with the MP group, and use of the website www.mantleplumes.org. Gillian Foulger is warmly thanked for the detailed comments, suggestions, and the punctual English text-sharpening process on several draft versions. Detailed reviews by Marjorie Wilson (Leeds, UK) and Erin Beutel (Charleston, USA) improved the quality of the manuscript.

REFERENCES CITED

Allegre, C.J., 1968, Comportement des systems U-Th-Pb dans le manteau supérieur et modèle d'évolution de cedernier au cours des temps géologiques: Earth and Planetary Science Letters, v. 5, p. 261–269, doi:10.1016/S0012-821X(68)80050-0.

Anderson, D.L., 1989, Where on Earth is the crust?: Physics Today, v. 42, p. 38–46, doi:10.1063/1.881215.

Anderson, D.L., 1995, Lithosphere, asthenosphere, and perisphere: Reviews of Geophysics, v. 33, p. 125–149, doi:10.1029/94RG02785.

Anderson, D.L., 1998, The helium paradoxes: Proceedings of the National Academy of Sciences of the United States of America, v. 95, p. 4822–4827, doi:10.1073/pnas.95.9.4822.

Anderson, D.L., 2007, New Theory of the Earth: Cambridge, UK, Cambridge University Press, 384 p., doi:10.1017/CBO9781139167291.

Anderson, D.L., 2011, Hawaii, boundary layers and ambient mantle—Geophysical constraints: Journal of Petrology, v. 52, p. 1547–1577, doi:10.1093/petrology/egq068.

Anderson, D.L., 2013, The persistent mantle plume myth: Australian Journal of Earth Sciences, v. 60, p. 657–673, doi:10.1080/08120099.2013.835283.

Anderson, D.L., and King, S.D., 2014, Driving the Earth machine?: Science, v. 346, p. 1184–1185, doi:10.1126/science.1261831.

Anderson, D.L., and Natland, J.H., 2014, Mantle updrafts and mechanisms of oceanic volcanism: Proceedings of the National Academy of Sciences of the United States of America, v. 111, p. E4298–E4304, doi:10.1073/pnas.1410229111.

Ballentine, C.J., 2012, A dash of deep nebula on the rocks: Nature, v. 486, p. 40–41, doi:10.1038/486040a.

Ballmer, M.D., Ito, G., Wolfe, C.J., and Solomon, S.C., 2013, Double layering of a thermochemical plume in the upper mantle beneath Hawaii: Earth and Planetary Science Letters, v. 376, p. 155–164, doi:10.1016/j.epsl.2013.06.022.

Birch, F., 1952, Elasticity and constitution of the Earth's interior: Journal of Geophysical Research, v. 57, p. 227–286.

Boehler, R., Chopelas, A., and Zerr, A., 1995, Temperature and chemistry of the core-mantle boundary: Chemical Geology, v. 120, p. 199–205.

Bolhar, R., Kamber, B.S., and Collerson, K.D., 2007, U-Th-Pb fractionation in Archaean lower continental crust: Implications for terrestrial Pb isotope systematics: Earth and Planetary Science Letters, v. 254, p. 127–145, doi:10.1016/j.epsl.2006.11.032.

Borisova, A.Yu., Belyatsky, B.V., Portnyagin, M.V., and Sushchevskaya, N.M., 2001, Petrogenesis of olivine-phyric basalts from the Aphanasey-Nikitin Rise: Evidence for contamination by cratonic lower continental crust: Journal of Petrology, v. 42, p. 277–319, doi:10.1093/petrology/42.2.277.

Bull, A.L., Domeier, M., and Torsvik, T.H., 2014, The effect of plate motion history on the longevity of deep mantle heterogeneities: Earth and Planetary Science Letters, v. 401, p. 172–182, doi:10.1016/j.epsl.2014.06.008.

Cadoux, A., Blichert-Toft, J., Pinti, D.L., and Albarède, F., 2007, A unique lower mantle source for southern Italy volcanics: Earth and Planetary Science Letters, v. 259, p. 227–238, doi:10.1016/j.epsl.2007.04.001.

Camp, V.E., 2013, Origin of Columbia River Basalt: Passive rise of shallow mantle or active upwelling of a deep-mantle plume?, *in* Reidel, S.P., Camp, V.E., Ross, M.E., Wolff, J.A., Martin, B.S., Tolan, T.L., and Wells, R.E., eds., The Columbia River Flood Basalt Province: Geological Society of America Special Paper 497, p. 181–199, doi:10.1130/2013.2497(07).

Campbell, I.H., and Griffiths, R.W., 2014, Did the formation of D″ cause the Archean-Proterozoic transition?: Earth and Planetary Science Letters, v. 388, p. 1–8, doi:10.1016/j.epsl.2013.11.048.

Cañón-Tapia, E., 2010, Origin of large igneous provinces: The importance of a definition, *in* Cañón-Tapia, E., and Szakács, A., eds., What Is a Volcano?: Geological Society of America Special Paper 470, p. 77–101, doi:10.1130/2010.2470(06).

Caro, G., and Bourdon, B., 2010, Non-chondritic Sm/Nd ratio in the terrestrial planets: Consequences for the geochemical evolution of the mantle-crust system: Geochimica et Cosmochimica Acta, v. 74, p. 3333–3349, doi:10.1016/j.gca.2010.02.025.

Carrol, M.R., and Draper, D.S., 1994, Noble gases as trace elements in magmatic processes: Chemical Geology, v. 117, p. 37–56.

Chauvel, C., Hofmann, A.W., and Vidal, P., 1992, HIMU-EM: The French Polynesian connection: Earth and Planetary Science Letters, v. 110, p. 99–119, doi:10.1016/0012-821X(92)90042-T.

Chauvel, C., Goldstein, S.L., and Hofmann, A.W., 1995, Hydration and dehydration of oceanic crust controls Pb evolution of the mantle: Chemical Geology, v. 126, p. 65–75, doi:10.1016/0009-2541(95)00103-3.

Class, C., and Goldstein, S.L., 2005, Evolution of helium isotopes in the Earth's mantle: Nature, v. 436, p. 1107–1112, doi:10.1038/nature03930.

Clift, P.D., and Vannucchi, P., 2004, Controls on the tectonic accretion versus erosion in subduction zones: Implications for the origin and recycling of the continental crust: Reviews of Geophysics, v. 42, RG2001, doi:10.1029/2003RG000127.

Cloetingh, S., Burov, E., and Francois, T., 2013, Thermo-mechanical controls on intra-plate deformation and the role of plume-folding interactions in continental topography: Gondwana Research, v. 24, p. 815–837, doi:10.1016/j.gr.2012.11.012.

Davies, G.F., 2011, Mantle Convection for Geologists: Cambridge, UK, Cambridge University Press, 232 p., doi:10.1017/CBO9780511973413.

DePaolo, D.J., Johnson, R.W., 1979, Magma genesis in the New Britain Island Arc: Constraints from Nd and Sr isotopes and trace-element patterns: Contributions to Mineralogy and Petrology, v. 70, p. 367–379.

Dupré, B., and Allègre, C.J., 1983, Pb–Sr isotope variation in Indian Ocean and mixing phenomena: Nature, v. 303, p. 142–146, doi:10.1038/303142a0.

Faccenna, C., and Becker, T.W., 2010, Shaping mobile belts by small-scale convection: Nature, v. 465, p. 602–605, doi:10.1038/nature09064.

Farnetani, C.G., and Richards, M.A., 1994, Numerical investigation of the mantle plume initiation model for flood basalt events: Journal of Geophysical Research, v. 99, p. 13,813–13,883, doi:10.1029/94JB00649.

Faure, G., and Powell, J.L., 1972, Strontium isotope geology: Berlin, Springer Verlag, 188 p., doi:10.1007/978-3-642-65367-4.

Fedele, L., Lustrino, M., Melluso, L., Morra, V., Zanetti, A., and Vannucci, R., 2015, Trace-element partitioning between plagioclase, alkali feldspar, Ti-magnetite, biotite, apatite and evolved potassic liquids from Campi Flegrei (Southern Italy): The American Mineralogist, v. 100, p. 233–249, doi:10.2138/am-2015-4995.

Foulger, G.R., 2010, Plates vs Plumes: A Geological Controversy: Chichester, UK, Wiley-Blackwell, 328 p.

Foulger, G.R., Panza, G.F., Artemieva, I.M., Bastow, I.D., Cammarano, F., Evans, J.R., Hamilton, W.B., Julian, B.R., Lustrino, M., Thybo, H., and Yanovskaya, T.B., 2013, Caveats on tomographic images: Terra Nova, v. 25, p. 259–281, doi:10.1111/ter.12041.

Fullea, J., Afonso, J.C., Connolly, J.A.D., Fernàndez, M., García-Castellanos, D., and Zeyen, H., 2009, LitMod3D: An interactive 3-D software to model the thermal, compositional, density, seismological and rheological structure of the lithosphere and sublithospheric upper mantle: Geochemistry Geophysics Geosystems, v. 10, Q08019, doi:10.1029/2009GC002391.

Gast, P.W., 1960, Limitations on the composition of the upper mantle: Journal of Geophysical Research, v. 65, p. 1287–1297, doi:10.1029/JZ065i004p01287.

Gast, P.W., 1968, Trace element fractionation and the origin of tholeiitic and alkaline magma types: Geochimica et Cosmochimica Acta, v. 32, p. 1057–1086, doi:10.1016/0016-7037(68)90108-7.

Glisovic, P., and Forte, A.M., 2014, Reconstructing the Cenozoic evolution of the mantle: Implications for mantle plume dynamics under the Pacific and Indian plates: Earth and Planetary Science Letters, v. 390, p. 146–156, doi:10.1016/j.epsl.2014.01.010.

Gonnermann, H.M., and Mukhopadhyay, S., 2009, Preserving noble gases in a convecting mantle: Nature, v. 459, p. 560–563, doi:10.1038/nature08018.

Graham, D.W., Larsen, L.M., Hanan, B.B., Storey, M., Pedersen, A.K., and Lupton, J.E., 1998, Helium isotope composition of the early Iceland mantle plume inferred from the Tertiary picrites of West Greenland: Earth and Planetary Science Letters, v. 160, p. 241–255, doi:10.1016/S0012-821X(98)00083-1.

Graham, D.W., Hanan, B.B., Hémond, C., Blichert-Toft, J., and Albarède, F., 2014, Helium isotopic textures in Earth's upper mantle: Geochemistry Geophysics Geosystems, v. 15, p. 2048–2074, doi:10.1002/2014GC005264.

Green, D.H., Hibberson, W.O., Kovács, I., and Rosenthal, A., 2010, Water and its influence on the lithosphere-asthenosphere boundary: Nature, v. 467, p. 448–451, doi:10.1038/nature09369.

Griffiths, R.W., and Campbell, I.H., 1990, Stirring and structure in mantle starting plumes: Earth and Planetary Science Letters, v. 99, p. 66–78, doi:10.1016/0012-821X(90)90071-5.

Gudfinnsson, G.H., and Presnall, D.C., 2005, Continuous gradations among primary carbonatitic, kimberlitic, melilititic, basaltic, picritic, and komatiitic melts in equilibrium with garnet lherzolite at 3–8 GPa: Journal of Petrology, v. 46, p. 1645–1659, doi:10.1093/petrology/egi029.

Gutenberg, B., 1959, Wave velocities below the Mohorovičić discontinuity: Geophysical Journal of the Royal Astronomical Society, v. 2, p. 348–352, doi:10.1111/j.1365-246X.1959.tb05805.x.

Hanyu, T., 2014, Deep plume origin of the Louisville hotspot: Noble gas evidence: Geochemistry Geophysics Geosystems, v. 15, p. 565–576, doi:10.1002/2013GC005085.

Hanyu, T., Clague, D.A., Kaneoka, I., Dunai, T.J., and Davies, G.R., 2005, Noble gas systematics of submarine alkalic lavas near the Hawaiian hotspot: Chemical Geology, v. 214, p. 135–155, doi:10.1016/j.chemgeo.2004.08.051.

Hanyu, T., Dosso, L., Ishizuka, O., Tani, K., Hanan, B.B., Adam, C., Nakai, S., Senda, R., Chang, Q., and Tatsumi, Y., 2013, Geochemical diversity in submarine HIMU basalts from Austral Islands, French Polynesia: Contributions to Mineralogy and Petrology, v. 166, p. 1285–1304, doi:10.1007/s00410-013-0926-x.

Hanyu, T., Kawabata, H., Tatsumi, Y., Kimura, J.-I., Hyodo, H., Sato, K., Miyazaki, T., Chang, Q., Hirahara, Y., Takahashi, T., Senda, R., and Nakai, S., 2014, Isotope evolution in the HIMU reservoir beneath St. Helena: Implications for the mantle recycling of U and Th: Geochimica et Cosmochimica Acta, v. 143, p. 232–252, doi:10.1016/j.gca.2014.03.016.

Hart, S.R., 1984, A large-scale isotope anomaly in the Southern Hemisphere mantle: Nature, v. 309, p. 753–757, doi:10.1038/309753a0.

Hart, S.R., 2014, Geochemical diversity of the mantle: 50 years of acronyms, *in* Proceedings, American Geophysical Union Fall Meeting, San Francisco, California, Abstract V22-B01.

Herzberg, C., 2011, Basalts as temperature probes of the Earth's mantle: Geology, v. 39, p. 1179–1180, doi:10.1130/focus122011.1.

Hirschmann, M.M., and Dasgupta, R., 2009, The H/C ratio of Earth's near-surface and deep reservoirs, and consequences for deep Earth volatile cycles: Chemical Geology, v. 262, p. 4–16, doi:10.1016/j.chemgeo.2009.02.008.

Hofmann, A.W., 1997, Mantle geochemistry: The message from oceanic volcanism: Nature, v. 385, p. 219–229, doi:10.1038/385219a0.

Hofmann, A.W., 2003, Sampling mantle heterogeneity through oceanic basalts: Isotopes and trace elements, *in* Carlson, R.W., Holland, H.D., and Turekian, K.K., eds., Treatise on Geochemistry, Volume 2: The Mantle and Core: Amsterdam, Springer, p. 61–101.

Hofmann, A.W., 2014, Fifty-one years of Hawaiian hotspot debate, *in* Proceedings, American Geophysical Union Fall Meeting, San Francisco, California, Abstract V23G-01.

Huang, S., and Frey, F.A., 2005, Recycled oceanic crust in the Hawaiian plume: Evidence from temporal geochemical variations within the Koolau shield: Contributions to Mineralogy and Petrology, v. 149, p. 556–575, doi:10.1007/s00410-005-0664-9.

Humphreys, E., and Schmandt, B., 2011, Looking for mantle plumes: Physics Today, v. 64, p. 34–39, doi:10.1063/PT.3.1217.

Ivanov, A.V., this volume, Why volatiles are required for cratonic flood basalt volcanism: Two examples from the Siberian craton, *in* Foulger, G.R., Lustrino, M., and King, S.D., eds., The Interdisciplinary Earth: A Volume in Honor of Don L. Anderson: Geological Society of America Special Paper 514 and American Geophysical Union Special Publication 71, doi:10.1130/2015.2514(19).

Jackson, C.R.M., Parman, S.W., Kelley, S.P., and Cooper, R.F., 2013, Constraints on light noble gas partitioning at the conditions of spinel-peridotite melting: Earth and Planetary Science Letters, v. 384, p. 178–187, doi:10.1016/j.epsl.2013.09.046.

Jackson, M.G., and Dasgupta, R., 2008, Compositions of HIMU, EM1, and EM2 from global trends between radiogenic isotopes and major elements in oceanic island basalts: Earth and Planetary Science Letters, v. 276, p. 175–186, doi:10.1016/j.epsl.2008.09.023.

Jackson, M.G., and Jellinek, A.M., 2013, Major and trace element composition of the high $^{3}He/^{4}He$ mantle: Implications for the composition of a non-chondritic Earth: Geochemistry Geophysics Geosystems, v. 14, p. 2954–2976, doi:10.1002/ggge.20188.

Jackson, M.G., Carlson, R.W., Kurz, M.D., Kempton, P.D., Francis, D., and Blusztajn, J., 2010, Evidence for the survival of the oldest terrestrial mantle reservoir: Nature, v. 466, p. 853–856, doi:10.1038/nature09287.

Jackson, M.G., Hart, S.R., Konter, J.G., Kurz, M.D., Blusztajn, J., and Farley, K.A., 2014, Helium and lead isotopes reveal the geochemical geometry of the Samoan plume: Nature, v. 514, p. 355–358, doi:10.1038/nature13794.

Jeanloz, R., and Morris, S., 1986, Temperature distribution in the crust and the mantle: Annual Review of Earth and Planetary Sciences, v. 14, p. 377–415.

Kawabata, H., Hanyu, T., Chang, Q., Kimura, J.-I., Nichols, A.R.L., and Tatsumi, Y., 2011, The petrology and geochemistry of St. Helena alkali basalts: Evaluation of the oceanic crust-recycling model for HIMU OIB: Journal of Petrology, v. 52, p. 791–838, doi:10.1093/petrology/egr003.

Kawakatsu, H., Kumar, P., Takei, Y., Shinohara, M., Kanazawa, T., Araki, E., and Suyehiro, K., 2009, Seismic evidence for sharp lithosphere-asthenosphere boundaries of oceanic plates: Science, v. 324, p. 499–502.

Keiding, J.K., Trumbull, R.B., Veksler, I.V., and Jerram, D.A., 2011, On the significance of ultra-magnesian olivines in basaltic rocks: Geology, v. 39, p. 1095–1098, doi:10.1130/G32214.1.

Keshav, S., and Gudfinnsson, G.H., 2014, Melting phase equilibria of model carbonated peridotite from 8 to 12 GPa in the system $CaO-MgO-A_{12}O_3-SiO_2-CO_2$ and kimberlitic liquids in the Earth's upper mantle: The American Mineralogist, v. 99, p. 1119–1126, doi:10.2138/am.2014.4826.

Lee, W.-J., Huang, W.L., and Wyllie, P., 2000, Melts in the mantle modeled in the system CaO-MgO-SiO2-CO2 at 2.7 GPa: Contributions to Mineralogy and Petrology, v. 138, p. 199–213, doi:10.1007/s004100050557.

Li, M., McNamara, A.K., and Garnero, E.J., 2014, Chemical complexity of hotspots caused by cycling oceanic crust through mantle reservoirs: Nature Geoscience, v. 7, p. 366–370, doi:10.1038/ngeo2120.

Litasov, K.D., 2011, Physicochemical conditions for melting in the Earth's mantle containing a C-O-H fluid (from experimental data): Russian Geology and Geophysics, v. 52, p. 475–492, doi:10.1016/j.rgg.2011.04.001.

Litasov, K.D., and Ohtani, E., 2003, Stability of various hydrous phases in CMAS pyrolite-H_2O system up to 25 GPa: Physics and Chemistry of Minerals, v. 30, p. 147–156, doi:10.1007/s00269-003-0301-y.

Lustrino, M., 2005, How the delamination and detachment of lower crust can influence basaltic magmatism: Earth-Science Reviews, v. 72, p. 21–38, doi:10.1016/j.earscirev.2005.03.004.

Lustrino, M., 2011, What 'anorogenic' igneous rocks can tell us about the chemical composition of the upper mantle: Case studies from the circum-Mediterranean area: Geological Magazine, v. 148, p. 304–316, doi:10.1017/S0016756810000695.

Lustrino, M., and Dallai, L., 2003, On the origin of EM-I end-member: Neues Jahrbuch für Mineralogie: Abhandlungen, v. 179, p. 85–100, doi:10.1127/0077-7757/2003/0179-0085.

Lustrino, M., and Wilson, M., 2007, The circum-Mediterranean anorogenic Cenozoic igneous province: Earth-Science Reviews, v. 81, p. 1–65, doi:10.1016/j.earscirev.2006.09.002.

Lyubetskaya, T., and Korenaga, J., 2007, Chemical composition of Earth's primitive mantle and its variance: 1. Methods and results: Journal of Geophysical Research, v. 112, B03211, doi:10.1029/2005JB004223.

Mahoney, J.J., and Coffin, M.F., eds., 1997, Large Igneous Provinces: Continental, Oceanic, and Planetary Flood Volcanism: American Geophysical Union Geophysical Monograph 100, 438 p., doi:10.1029/GM100.

Mahoney, J.J., White, W.M., Upton, B.G.J., Neal, C.R., and Scrutton, R.A., 1996, Beyond EM-1: Lavas from Afanasy-Nikitin Rise and the Crozet Archipelago, Indian Ocean: Geology, v. 24, p. 615–618, doi:10.1130/0091-7613(1996)024<0615:BELFAN>2.3.CO;2.

Mallik, A., and Dasgupta, R., 2014, Effect of variable CO_2 on eclogite-derived andesite and lherzolite reaction at 3 GPa—Implications for mantle source characteristics of alkalic island basalts: Geochemistry Geophysics Geosystems, v. 15, p. 1533–1557, doi:10.1002/2014GC005251.

McKenzie, D., and Bickle, M.J., 1988, The volume and composition of melt generated by extension of the lithosphere: Journal of Petrology, v. 29, p. 625–679, doi:10.1093/petrology/29.3.625.

Meibom, A., Anderson, D.L., Sleep, N.H., Frei, R., Page Chamberlain, C., Hren, M.T., and Wooden, J.L., 2003, Are high $^3He/^4He$ ratios in oceanic basalts an indicator of deep-mantle plume components?: Earth and Planetary Science Letters, v. 208, p. 197–204, doi:10.1016/S0012-821X(03)00038-4.

Merle, R., Jourdan, F., Marzoli, A., Renne, P.R., Grange, M., and Girardeau, J., 2009, Evidence of multi-phase Cretaceous to Quaternary alkaline magmatism on Tore-Madeira Rise and neighbouring seamounts from $^{40}Ar/^{39}Ar$ ages: Journal of the Geological Society, v. 166, p. 879–894, doi:10.1144/0016-76492008-060.

Montelli, R., Nolet, G., Dahlen, F.A., Masters, G., Engdahl, R., and Hung, S.-H., 2004, Finite-frequency tomography reveals a variety of plumes in the mantle: Science, v. 303, p. 338–343, doi:10.1126/science.1092485.

Moreira, M., Kanzari, A., and Madureira, P., 2012, Helium and neon isotopes in São Miguel island basalts, Azores archipelago: New constraints on the "low ^3He" hotspot origin: Chemical Geology, v. 322–323, p. 91–98, doi:10.1016/j.chemgeo.2012.06.014.

Morgan, W.J., 1971, Convection plumes in the lower mantle: Nature, v. 230, p. 42–43, doi:10.1038/230042a0.

Morgan, W.J., 1972, Deep mantle convection plumes and plate motions: American Association of Petroleum Geologists Bulletin, v. 56, p. 203–213.

Mourão, C., Moreira, M., Mata, J., Raquin, A., and Madeira, J., 2012, Primary and secondary processes constraining the noble gas isotopic signatures of carbonatites and silicate rocks from Brava Island: Evidence for a lower mantle origin of the Cape Verde plume: Contributions to Mineralogy and Petrology, v. 163, p. 995–1009, doi:10.1007/s00410-011-0711-7.

Nakagawa, T., and Tackley, P.J., 2014, Influence of combined primordial layering and recycled MORB on the coupled thermal evolution of Earth's mantle and core: Geochemistry Geophysics Geosystems, v. 15, p. 619–633, doi:10.1002/2013GC005128.

Natland, J.H., 2003, Capture of helium and other volatiles during the growth of olivine phenocrysts in picritic basalts from the Juan Fernandez Islands: Journal of Petrology, v. 44, p. 421–456, doi:10.1093/petrology/44.3.421.

Niu, Y., and O'Hara, M.J., 2008, Global correlations of ocean ridge basalt chemistry with axial depth: A new perspective: Journal of Petrology, v. 49, p. 633–664, doi:10.1093/petrology/egm051.

Niu, Y., Wilson, M., Humphreys, E.R., and O'Hara, M.J., 2011, The origin of intraplate island basalt (OIB): The lid effect and its geodynamic implications: Journal of Petrology, v. 52, p. 1443–1468, doi:10.1093/petrology/egr030.

Nixon, P.H., ed., 1987, Mantle Xenoliths: New York, John Wiley & Sons Ltd., 864 p.

Ozima, M., and Igarashi, G., 2000, The primordial noble gases in the Earth: A key constraint on Earth evolution models: Earth and Planetary Science Letters, v. 176, p. 219–232, doi:10.1016/S0012-821X(00)00005-4.

Papanastassiou, D.A., and Wasserburg, G.J., 1969, Initial Sr isotopic abundances and the resolution of small time differences in the formation of planetary objects: Earth and Planetary Science Letters, v. 5, p. 361–376.

Parman, S.W., Kurz, M.D., Hart, S.R., and Grove, T.L., 2005, Helium solubility in olivine and implications for high $^3He/^4He$ in ocean island basalt: Nature, v. 437, p. 1140–1143, doi:10.1038/nature04215.

Pearson, D.G., Brenker, F.E., Nestola, F., McNeill, J., Nasdala, L., Hutchison, M.T., Matveev, S., Mather, K., Silversmit, G., Schmitz, S., Vekemans, B., and Vincze, L., 2014, Hydrous mantle transition zone indicated by ringwoodite included within diamond: Nature, v. 507, p. 221–224, doi:10.1038/nature13080.

Peters, B.J., and Day, J.M.D., 2014, Assessment of relative Ti, Ta and Nb (TITAN) enrichments in ocean island basalts: Geochemistry Geophysics Geosystems, v. 15, p. 4424–4444, doi:10.1002/2014GC005506.

Pfander, J.A., Jung, S., Münker, C., Stracke, A., and Mezger, K., 2012, A possible high Nb/Ta reservoir in the continental lithospheric mantle and consequences on the global Nb budget—Evidence from continental basalts from central Germany: Geochimica et Cosmochimica Acta, v. 77, p. 232–251, doi:10.1016/j.gca.2011.11.017.

Pilet, S., this volume, Generation of low-silica alkaline lavas: Petrological constraints, models and thermal implications, *in* Foulger, G.R., Lustrino, M., and King, S.D., eds., The Interdisciplinary Earth: A Volume in Honor of Don L. Anderson: Geological Society of America Special Paper 514 and American Geophysical Union Special Publication 71, doi:10.1130/2015.2514(17).

Pilet, S., Baker, M.B., Müntener, O., and Stolper, E.M., 2011, Monte Carlo simulations of metasomatic enrichment in the lithosphere and implications for the source of alkaline basalts: Journal of Petrology, v. 52, p. 1415–1442, doi:10.1093/petrology/egr007.

Plank, T., 2014, The chemical composition of subducting sediments, *in* Holland, H.D., and Turekian, K.K., eds., Treatise on Geochemistry (2nd edition), Volume 4: The Crust: Amsterdam, Elsevier, p. 607–629, doi:10.1016/B978-0-08-095975-7.00319-3.

Prelevic, D., and Foley, S.F., 2007, Accretion of arc-oceanic lithospheric mantle in the Mediterranean: Evidence from extremely high-Mg olivines and Cr-rich spinel inclusions in lamproites: Earth and Planetary Science Letters, v. 256, p. 120–135, doi:10.1016/j.epsl.2007.01.018.

Presnall, D.C., and Gudfinnsson, G.H., 2011, Oceanic volcanism from the Low-Velocity Zone - without mantle plumes: Journal of Petrology, v. 52, p. 1533–1546.

Putirka, K.D., 2005, Mantle potential temperatures at Hawaii, Iceland, and the mid-ocean ridge system, as inferred from olivine phenocrysts: Evidence for thermally driven mantle plumes: Geochemistry Geophysics Geosystems, v. 6, Q05L08, doi:10.1029/2005GC000915.

Putirka, K.D., Perfit, M., Ryerson, F.J., and Jackson, M.G., 2007, Ambient and excess mantle temperatures, olivine thermometry and active vs. passive upwelling: Chemical Geology, v. 241, p. 177–206.

Ringwood, A.E., 1979, Composition and Origin of the Earth: New York, Springer Verlag, 295 p., doi:10.1007/978-1-4612-6167-4.

Salters, V.J.M., and Sachi-Kocher, A., 2010, An ancient metasomatic source for the Walvis Ridge basalts: Chemical Geology, v. 273, p. 151–167, doi:10.1016/j.chemgeo.2010.02.010.

Sandwell, D.T., Müller, R.D., Smith, W.H.F., Garcia, E., and Francis, R., 2014, New global marine gravity model from CryoSat-2 and Jason-1 reveals buried tectonic structure: Science, v. 346, p. 65–67, doi:10.1126/science.1258213.

Schmidt, M.W., and Poli, S., 2014, Devolatilization during subduction, *in* Rudnick, R.L., ed., Treatise on Geochemistry (2nd edition), Volume 4: The Crust: Amsterdam, Elsevier, p. 669–701, doi:10.1016/B978-0-08-095975-7.00321-1.

Schuberth, B.S.A., Bunge, H.-P., Steinle-Neumann, G., Moder, C., and Oeser, J., 2009, Thermal versus elastic heterogeneity in high-resolution mantle circulation models with pyrolite composition: High plume excess temperatures in the lowermost mantle: Geochemistry Geophysics Geosystems, v. 10, Q01W01, doi:10.1029/2008GC002235.

Shorttle, O., Maclennan, J., and Lambart, S., 2014, Quantifying lithological variability in the mantle: Earth and Planetary Science Letters, v. 395, p. 24–40.

Smith, A.D., this volume, A perisphere/LLAMA model for Hawaiian volcanism, *in* Foulger, G.R., Lustrino, M., and King, S.D., eds., The Interdisciplinary Earth: A Volume in Honor of Don L. Anderson: Geological Society of America Special Paper 514 and American Geophysical Union Special Publication 71, doi:10.1130/2015.2514(18).

Sobolev, S.V., Sobolev, A.V., Kuzmin, D.V., Krivolutskaya, N.A., Petrunin, A.G., Arndt, N.T., Radko, V.A., and Vasiliev, Y.R., 2011, Linking mantle plumes, large igneous provinces and environmental catastrophes: Nature, v. 477, p. 312–316, doi:10.1038/nature10385.

Stracke, A., 2012, Earth's heterogeneous mantle: A product of convection-driven interaction between crust and mantle: Chemical Geology, v. 330–331, p. 274–299, doi:10.1016/j.chemgeo.2012.08.007.

Stracke, A., Hofmann, A.W., and Hart, S.R., 2005, FOZO, HIMU, and the rest of the mantle zoo: Geochemistry Geophysics Geosystems, v. 6, Q05007, doi:10.1029/2004GC000824.

Stuart, F.M., Lass-Evans, S., Fitton, J.G., and Ellam, R.M., 2003, High $^{3}He/^{4}He$ ratios in picritic basalts from Baffin Island and the role of a mixed reservoir in mantle plumes: Nature, v. 424, p. 57–59, doi:10.1038/nature01711.

Tanaka, R., Nakamura, E., and Takahashi, E., 2002, Geochemical evolution of Koolau Volcano, Hawaii, *in* Takahashi, E., Lipman, P.W., Garcia, M.O., Naka, J., and Aramaki, S., eds., Hawaiian Volcanoes: Deep Underwater Perspectives: American Geophysical Union Geophysical Monograph 128, p. 311–332, doi:10.1029/GM128p0311.

Tatsumoto, M., 1978, Isotopic composition of lead in oceanic basalt and its implication to mantle evolution: Earth and Planetary Science Letters, v. 38, p. 63–87, doi:10.1016/0012-821X(78)90126-7.

Vitale Brovarone, A., and Beyssac, O., 2014, Lawsonite metasomatism: A new route for water to the deep Earth: Earth and Planetary Science Letters, v. 393, p. 275–284, doi:10.1016/j.epsl.2014.03.001.

White, W.M., 2010, Oceanic island basalts and mantle plumes: The geochemical perspective: Annual Review of Earth and Planetary Sciences, v. 38, p. 133–160, doi:10.1146/annurev-earth-040809-152450.

Willbold, M., and Stracke, A., 2010, Formation of enriched mantle components by recycling of upper and lower continental crust: Chemical Geology, v. 276, p. 188–197, doi:10.1016/j.chemgeo.2010.06.005.

Wilson, T.J., 1963, A possible origin of the Hawaiian islands: Canadian Journal of Physics, v. 41, p. 863–870.

Woodhead, J.D., and Devey, C.W., 1993, Geochemistry of the Pitcairn seamounts, I: Source character and temporal trends: Earth and Planetary Science Letters, v. 116, p. 81–99, doi:10.1016/0012-821X(93)90046-C.

Zindler, A., and Hart, S., 1986, Chemical geodynamics: Annual Review of Earth and Planetary Sciences, v. 14, p. 493–571, doi:10.1146/annurev.ea.14.050186.002425.

Manuscript Accepted by the Society 2 February 2015
Manuscript Published Online 20 August 2015

Printed in the USA

Geological Society of America Special Papers

The mantle isotopic printer: Basic mantle plume geochemistry for seismologists and geodynamicists

Michele Lustrino and Don L. Anderson

Geological Society of America Special Papers 2015;514; 257-279 , originally published onlineAugust 20, 2015
doi:10.1130/2015.2514(16)

Notes